RESEARCH PAPER

Investigation of the anti-inflammatory efficacy of selected homeopathic formulation through CFA-induced arthritis, accompanied by an in silico analysis

Bharati Gawai[1], Amol A. Tagalpallewar[1], Dipshikha Basangar[2], Shuchi Nagar[2]* and Akshay M. Baheti[1]*

[1]*Department of Pharmaceutical Sciences, School of Health Sciences and Technology, Dr.Vishwanath Karad MIT World Peace University, Pune, Maharashtra, India*
[2]*Bioinformatics Centre, Dr. D. Y. Patil Biotechnology & Bioinformatics Institute, Dr. D. Y. Patil Vidyapeeth, Pune, Maharashtra, India*
[1] *Orchid id: 0009-0008-7987-4830*
Corresponding Author: *akshay.baheti@mitwpu.edu.in, shuchisn@gmail.com*

Received: 24th April, 2026; Revised: 20th May 2026; Accepted: 30th June, 2026; Available Online: 10th July, 2026

ABSTRACT

Background and Aim:
Increased inflammatory cytokines, oxidative stress, and joint destruction are associated with rheumatoid arthritis, a chronic autoimmune inflammatory disease. Investigating the anti-arthritic potential of Bryonia alba mother tincture (BHMT) and its homoeopathic dilutions (6CH, 30CH, and 200CH) utilizing molecular dynamics simulation, HRLCMS profiling, in silico research, ADMET analysis, and in vivo testing in rats with CFA-induced arthritis.

Material and methods:
The phytoconstituents in BHMT and its dilutions were identified by HR-LCMS analysis. Following molecular docking against inflammatory targets such as TNF-α, COX-1, COX-2, and 15-lipoxygenase-2, the identified compounds underwent molecular dynamics modeling and ADMET prediction. In Wistar rats with arthritis induced by Complete Freund's Adjuvant (CFA), anti-arthritic activity was assessed by measuring paw edema, oxidative stress markers (SOD, CAT, GSH, MDA), pro-inflammatory cytokines (TNF-α and IL-6), and radiographic and histological alterations.

Results:
Several phytoconstituents in BHMT and their potencies were found by HR-LCMS analysis. With binding scores that were on the same level as or higher than Diclofenac, Discadenine and Bowdichione demonstrated a considerable docking affinity toward inflammatory proteins. While ADMET experiments revealed advantageous pharmacokinetic characteristics, MD modeling verified stable protein–ligand interactions. Bryonia alba formulations, especially 30CH and 200CH, were shown to have strong anti-arthritic action in in vivo experiments. Antioxidant properties were restored, radiographic and histological abnormalities were improved, paw edema was decreased, and TNF-α and IL-6 levels were decreased. The outcomes were comparable to those of receiving diclofenac.

Conclusion:
Bryonia alba has significant anti-inflammatory and anti-arthritic potential, according to the study. While in vivo results showed increased biological activity in potentized formulations, particularly 30CH and 200CH, HR-LCMS, docking, and MD modeling confirmed the medicinal importance of phytoconstituents contained in the mother tincture. These results encourage deeper investigation into the molecular processes of potentized drugs and propose that further homeopathic potentization studies are required to understand the biological responses.

**Author for Correspondence: akshay.baheti@mitwpu.edu.in*

GRAPHICAL REPRESENTATION

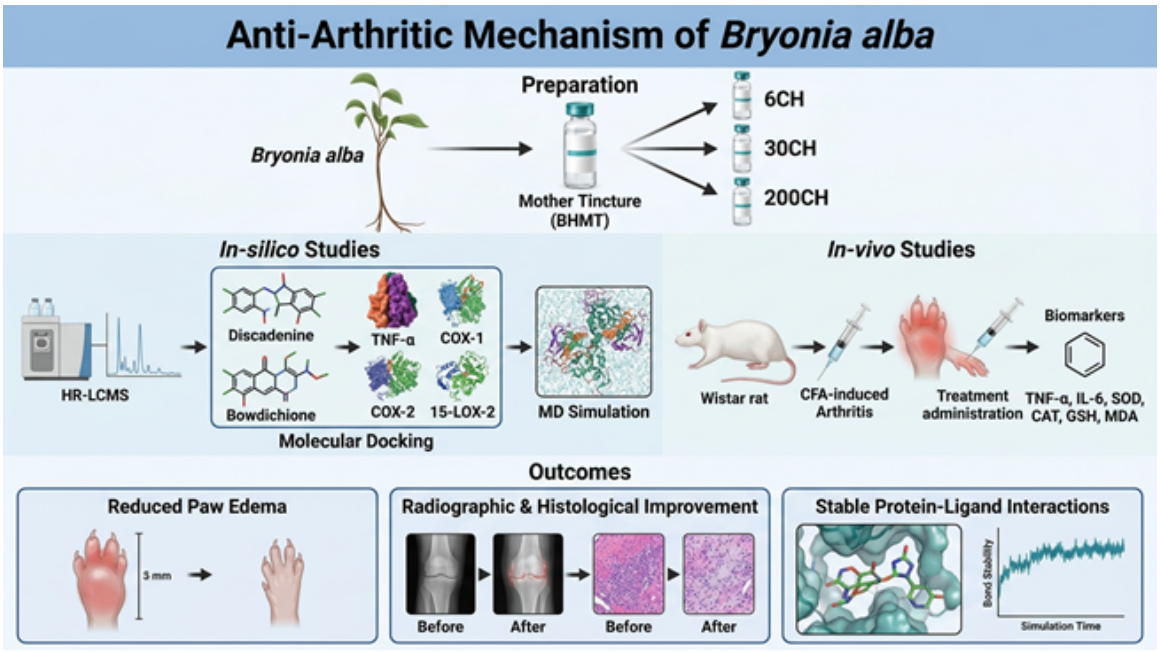

ABBREVIATIONS LIST

ADMET: Absorption, Distribution, Metabolism, Excretion, and Toxicology

CAT: Catalase

COX: Cyclooxygenase

B6CH: *Bryonia Alba* 6 Centesimal Hahnemannian

B30CH: *Bryonia Alba* 30 Centesimal Hahnemannian

B200CH: *Bryonia Alba* 200 Centesimal Hahnemannian

BHMT: *Bryonia Alba* Homeopathic Mother Tincture

GSH: glutathione

HRLC-MS: High Resolution Liquid Chromatography- Mass Spectrometry

LPO: Lipid peroxidase

NSAIDs: Nonsteroidal Antinflammatory Drugs

SOD: Superoxide dismutase

TNF: Tumor Necrosis Factor

MD simulation: Molecular dynamics

Keywords: *Anti-inflammatory, Bryonia Alba, Homeopathy, in-silico, potency*

How to cite this article: Gawai B, Tagalpallewar AA, Basangar D, Nagar S, Baheti AM., Investigation of the anti-inflammatory efficacy of selected homeopathic formulation through CFA-induced arthritis, accompanied by an in silico analysis. Int J Drug Deliv Technol. 2026;16(76s): 1709-1733; DOI: 10.25258/ijddt.16.76s.162
Source of support: Nil.
Conflict of interest: None

1. INTRODUCTION

Rheumatoid arthritis is a long term immune-mediated chronic disorder characterized by joint pain, stiffness, and swelling. Joint issues may coexist with systemic symptoms like fever, weight loss, and exhaustion. In the pathophysiology of RA, immune cells like fibroblasts and macrophages are activated and release cytokines like IL-6 and TNF-α. Tissue deterioration brought on by RA may result in joint deformity and chronic pain. Treatment approaches that have been demonstrated to control RA include nonsteroidal anti-inflammatory drugs (NSAIDs), biologic therapy that targets specific cytokines, and

disease-modifying antirheumatic pharmaceuticals (DMARDs) (1).

It has been known that rheumatoid arthritis, an inflammatory condition with an unknown cause, has occurred since at least the 1800s (2). The development of this progressive and frequently life-threatening condition can be delayed or stopped by prompt diagnosis and the initial start of absolute disease-modifying treatment, according to recent data. This permits patients to preserve function that they might normally lose. Chronic inflammatory disorders can be treated by a number of medications, but long-term use of these medications should be avoided because of their serious adverse effects (3).

Homoeopathy, a holistic therapeutic approach developed by Hahnemann in 1796, is based on the theory that illnesses can be cured with small portion of medications that can produce similar signs in healthy people. A process called "potentization" strengthens a medicine when it is diluted; often, pharmaceuticals are extensively diluted beyond the scope of molecular biology (4–7). By minimizing over-activation of the immune cascade, homoeopathy can decrease the progression of disease. This can have an impact on the host immune response, cytokine induction, and gene expression (8–10). The comprehensive approach to patient care known as "individualized homeopathy" takes into account a patient's clinical appearance, pathologies, physiological traits, and individual emotional responses previous illnesses that may signal comorbidities, and premorbid health evaluation. One recommended homeopathic drug that enhances the patient's illness is given as part of the treatment (11). Potentization is a basic method in homeopathy that creates potentized dilutions or potencies by gradually diluting mother tinctures or ethanolic solutions made from crude medications and then subjecting them to forceful hitting and vigorous shaking, a process known as succussion (12). The centesimal (C) scale, which uses dilution by a factor of 100 at each level, is used to define the majority of homeopathic medications. This method has been used six times with a 6C potency, yielding a dilution rate of one part in 10^6; thirty times with a 30C potency, yielding a dilution rate of one part in 10^{30} (13,14). Perennial plants with annual climbing or trailing stems are found in the genus Bryonia L. (Cucurbitaceae). Turkey's flora has four species of the Bryonia genus: Bryonia multiflora, Bryonia cretica, Bryonia aspera, and Bryonia alba. Because of its traditional use, B. alba L. was chosen as a material for this investigation. B. alba stems are often glandular, occasionally hairy or sparsely spiculate, and irregularly glabrous. The plant has thin to broad ovate-cordate leaves. B. alba has smooth or hardly pointed leafstalks. For a very long time, bryonia species have historically been used as diuretics and laxatives to alleviate swelling, edema, and joint discomfort. Because of their medicinal properties, B. alba roots are applied to aching joints and used specifically to alleviate rheumatic pain (15–17). Traditional medicine also uses the roots to treat rheumatism, pneumonia, and cough because they have a calming effect on oedema of the serous tissues. (18,19). A multi-target bioactive substance with anti-inflammatory, antioxidant, antipyretic, antibacterial, larvicidal, and cytotoxic qualities is another biological impact of bryonia species (20). Both cytotoxic and anticancer characteristics are included in their components.

2. MATERIALS AND EXPERIMENTAL METHODS

2.1 Experimental Chemicals and Reagents.

Bryonia alba preparations at different homeopathic dilutions of 6C, 30C, and 200C, along with ethanol as 90%, obtained from Hahnemann Publishing Co. Pvt. Ltd., India. The mother tincture of *Bryonia alba* and its corresponding potencies (6CH, 30CH, and 200CH; Batch Nos. 0466015, 0751648, 0572198, and 0572854) were sourced via the official portal of Dr. Willmar Schawabe India, Pune. Diclofenac sodium (Batch No. JS1273) was supplied by JB Chemicals, while Complete Freund's Adjuvant (CFA) (Sigma-Aldrich, Lot no. SLCH4887) was procured for experimental use. Enzyme-linked immunosorbent assay (ELISA) kits specific for rat TNF-α (DEVELOP, Lot no. EDL2025060304) and IL-6 (DEVELOP, Lot no. EDL2025021203) was utilized to quantify cytokines.

2.2 High Resolution Liquid Chromatography -Mass Spectroscopy (HRLC-MS/MS) study

The bioactive compounds were identified by HR-LCMS analysis of BHMT, B6CH, B30CH, and B200CH at the Sophisticated Analytical Instrument Facility (SAIF), IIT Bombay, Mumbai, India. High-resolution liquid chromatography–mass spectrometry (HRLC-MS) study was carried out using a Vanquish UHPLC system and a Thermo Scientific Q ExactiveTM Plus Orbitrap mass spectrometer. Thermo Scientific SII Xcalibur software was applied for instrument control and data acquisition, and Compound DiscovererTM was utilized for spectral interpretation and processing. Chromatographic separation was accomplished by using a reverse-phase C18 analytical column (100 × 2.1 mm, 1.7 µm) in a section of a thermostat column maintained at 40 °C. A high-precision auto-sampler (G4226A HiP Sampler) was used to introduce the samples (5.0 µL) in full-loop injection mode. To reduce carryover, pre- and post-injection needle washing was enabled. The mobile phase was composed of Solvent D, which was 95% acetonitrile (ACN) with 0.1% formic acid, and Solvent A, it was Milli-Q water with 0.1% formic acid. The gradient was set up in this way: For a total run length of 35 minutes, the system ramped up to 95% D (20–25 minutes), held for 5 minutes, then re-equilibrated to 5% D after 30 minutes. The maximum operational backpressure limit was set at 1200 bar, and the flow rate was kept at 0.30 mL/min. Using a Dual AJS ESI source, mass spectrometric detection was carried out in positive electrospray ionization (ESI) mode with the following setting: capillary voltage, 3500 V; nozzle voltage, 1000 V; sheath gas temperature, 300 °C; drying gas temperature, 250 °C; sheath gas flow, 11 L/min; nebulizer pressure, 35

psi; and fragmentor voltage, 175 V. Following 70,000 FWHM resolution MS1 acquisition (AGC target: 3×10^6; scan range: m/z 70–1000), data-dependent MS/MS (dd-MS^2) scans were run at 17,500 resolutions with a stepped normalized collision energy (NCE) of 30. There must be no more than 10 precursors every cycle, and dynamic exclusion was set at 10 s.

2.3. *In-silico* study

2.3.1. Ligand preparation:

The phytoconstituents identified by high resolution liquid chromatography–mass spectrometry (HRLC-MS) in BHMT, B6CH, B30CH, B200CH were selected for this study. These compounds' (ligands') three-dimensional (3D) chemical structures were obtained in Structure Data File (SDF) format from the PubChem database (https://pubchem.ncbi.nlm.nih.gov/) and used for a molecular docking study (21,22). To achieve energetically stable conformations appropriate for computational modeling, all ligand compounds underwent geometry optimization using Maestro software (version 13.4, Schrödinger LLC) prior to docking (23).

2.3.2 Protein preparation:

UniProt database (https://www.uniprot.org/) (24), Targets for proteins associated with inflammatory pathways were found, such as 15-lipoxygenase-2 (PDB ID: 7LAF), Cyclooxygenase-1 (COX-1; PDB ID: 5F1A), Cyclooxygenase-2 (COX-2; PDB IDs: 4XUM, 5IKR), and tumor necrosis factor-α (TNF-α; PDB IDs: 3APC, 3FMK, 5OQW). In order to guarantee superior geometry and improved visualization, option of Protein Preparation Wizard in Schrödinger Maestro (version 13.4) served to refine the conformation of each protein (25). Using Flex X Lead IT, docking experiments and binding site prediction were carried out to describe protein–ligand interactions and find active site residues. Analysis of interactions was prioritized for amino acid residues that were found within the expected binding pockets during virtual screening (26,27).

2.3.3. Molecular docking study:

Molecular docking was carried out utilising the Lead IT 2.3.2 application on the Flex-X for the virtual screening of ligands. (Flex-X Version 2.2.0) platform (28). The ligand molecules were permitted to display flexibility during docking, but the protein was kept in a rigid condition. After the ligands were docked with the proteins 15-lipoxygenase-2 (PDB ID 7LAF), COX-1 (PDB ID 5F1A), Cox-2 (PDB ID 4XUM, 5IKR), TNF-alpha (PDB ID 3APC, 3FMK, 5OQW), the results were assessed using Lead IT's best posture. During the docking process at the binding site, numerous potential ligand conformations and combinations were created. By comparing the ligands to the reference molecule, Diclofenac. the ligands were screened using the docking score and binding interactions.

2.3.4. Molecular dynamics simulation study:

MD simulations were performed using module of Schrödinger's Desmond to determine the stability of the binding interactions between the selected medications and proteins in a specific solvent environment. The docked protein–ligand complexes that served as input structures were prepared using Desmond's system setup program. he systems were solvated using the TIP3P water model and then neutralized by accumulation of Na^+ and Cl^- ions. Once system setup, energy minimization, equilibration was performed under NPT circumstances using Desmond's as default relaxation approach. Molecular dynamic simulations in the NPT ensemble under periodic boundary conditions were then performed using the OPLS3 force field. (Schrodinger Release 2022-3: Desmond Molecular Dynamics System, D. E. Shaw Research, New York, NY, USA, 2022) Initially, Maestro's Desmond System Builder program was used to build the docking complexes for the runs. The simulations were carried out in an orthorhombic box containing specific water molecules produced by the TI3P mode (31). Prior to the MD simulations, the components were minimized using the OPLS3 (optimal potential for liquid simulations) the force field approach to avoid steric conflicts. Once the settings were complete, Desmond's Molecular Dynamics interface was used to load simulations for one hundred ns runs (32). Each MD simulation began with A 24 ps-long NPT collective simulation at 300 K temperature and 1.01325 bar pressure, two 12 ps-long NPT ensemble simulations at 10 K temps and 1.01325 bar pressure, and a 12 ps-long NVT ensemble simulation at 10 K temp. Equilibration using the default settings was also part of the typical relaxation process (33,34). Following the relaxation, all MD simulations were conducted under NPT conditions at 300 K and 1.01325 bar (35). Furthermore, the trajectory's recording interval was set to 1000 ps, which might make it more difficult to fully analyze quick chemical occurrences. Temperature and pressure were controlled using the Martyna-Tobias-Klein barostat and the Nose-Hoover chain thermostat (36),(37). The 1002 frames that were recorded during the experiment were assessed using Desmond's experiment Interaction Diagram tool. The RMSD of frame X was obtained using the following formula

$$\mathrm{RMSD_x} = \sqrt{\frac{1}{N}\sum_{i=1}^{N}\left(r_i'(t_x)\right) - r_i\left(t_{ref}\right)\Big)^2}$$

where r is the position of the chosen atoms in a frame x after superposition on the reference frame, where frame x is recorded at time tx, N is the number of atoms in the atom selection, and t ref is the reference time (usually the first frame is used as the reference and is regarded as time t = 0). For each frame in the simulation trajectory, the process was carried out. The following formula was used to determine the RMSF for residue I.:

$$\mathrm{RMSF_i} = \sqrt{\frac{1}{T}\sum_{t=1}^{T} < \left(r_i'(t_x)\right) - r_i\left(t_{ref}\right)\Big)^2 >}$$

where rti is the atomic position of residue I, r is the position of atoms in residue I after superposition on the

reference, and T is the trajectory of the time over which the RMSF is computed. The average square distance is computed over the residue's atom selection, as indicated by the angle brackets.

2.3.5. ADMET Study

Absorption, Distribution, Metabolism, Excretion, and Toxicology (ADMET) evaluation helps reduce potential risks throughout clinical development. The Swiss-ADME server was used to perform the ADMET analysis. For research, the ADMET lab 2.0 in silico web server (https://admetmesh.scbdd.com/) was utilized. Furthermore, "Lipinski rule of Five" applied in the Swiss ADME (http://www.swissadme.ch/) web-based application to assess the constituents' ability to function as a medication (22,38).

3. *In-vivo* study

3.1. Animals

For the investigation on CFA-induced arthritis, mature Wistar albino rats of both male and female weighing in range of 200 and 250 g stayed chosen after the ADMET evaluation. The mice were housed in standard laboratory cages with a controlled 12-hour day and a 12-hour night cycle. The room was maintained at a temperature of 20 to 23 °C and a relative humidity of 30 to 70%. Each rat was given unrestricted access to a standard laboratory diet from VRK Nutritional Solutions, Sangli, India, while autoclaved maize cobs served as bedding. The Institutional Animal Ethics Committee examined and approved the experimental methods under protocol number 2166/PO/RcBi/S/22CPCSEA.

3.2. Administration of doses

In accordance with respective treatment groups, 0.1 ml of BHMT, B6CH, B30CH, and B200CH was each diluted with 1 ml of sterile water for injection and administered orally. A 0.1 ml dose of a 1% w/v CFA injection was given 1 hour before BHMT, B6CH, B30CH, and B200CH administration. Diclofenac (5 mg/kg, p.o.) was administered 1 hour before the CFA injection as the standard reference anti-inflammatory medication.

3.3. Experimental design

Rats were randomly assigned to five groups of six and given CFA injections to induce arthritis. Group 1 did not receive any therapy and served as the normal control (NC). To cause inflammation, groups 2 through 7 were given a subcutaneous injection of 0.1 ml of 1% w/v CFA (Freund's complete adjuvant) into the plantar side of the left hind paw. Group 2 did not receive any treatment and was the disease control (DC). Group 3, the standard control (SC), was given Diclofenac (5 mg/kg). Groups 4 (BHMT), 5 (B6CH), 6 (B30CH), and 7 (B200CH) were action groups and given 0.1 ml doses of BHMT, B6CH, B30CH, and B200CH, respectively. Rats were fasted overnight before treatment. Immediately after injection, the paw was marked with ink. Paw volumes were measured using plethysmography (Orchid Scientific, India). Paw edema was regularly observed on days 0, 7, 14, 21, and 28. Blood sample collection was done on the last day to estimate serum cytokines. BHMT was tested in concentrated form at 6CH, 30CH, and 200CH. Treatments lasted for 28 days and were given daily. Blood (0.4–0.6 mL) was drawn on the final day and aliquoted in 1.5 ml tubes of eppendorf. The serum was extracted and centrifuged at 10,000 rpm for 15 minutes. This serum was used to measure lipid peroxidation, antioxidant parameters (SOD, CAT, and GSH), and pro-inflammatory cytokines (TNF-alpha and IL-6). After blood collection, radiological analysis was performed (Edusoft Healthcare Pvt Ltd, India).

Lipid peroxidation (LPO) (39), glutathione (40), superoxide dismutase (41), and catalase (42) were assessed to be present in the serum. ELISA kits 96T were used to test the amounts of TNF-α and IL-6 in the serum sample.

3.4. Statistical analysis

The mean ± Standard Error of Mean (SEM) is employed to express values. Student's t-test was used to compare the disease control, normal control groups in order to assess statistical significance. One-way analysis of variance (ANOVA) and Dunnett's comparison test were utilised to contrast the drug-treated and disease-control groups. When $p < 0.05$, the results were deemed significant.

4. Results

4.1 HR-LCMS analysis

BHMT and its diluents B6CH, B30CH, B200CH, in all have 48 constituents detected by HR-LCMS analysis (Table 1).

Table no.1 List of components retrieved during HR-LCMS analysis of an BHMT, B6CH, B30CH, B200CH

Compounds	Retention Time (Min)	Molecular Weight	Molecular Formula
BHMT			
Ganoderic acid beta	9.139	496.293	C30 H44 O6
Cucurbitacin S	9.404	498.2974	C30 H42 O6
Anabsinthin	10.302	496.2834	C30 H40 O6
Polyporusterone C	8.116	476.315	C28 H44 O6
Polyporusterone D	8.721	460.3198	C28 H44 O5
Pubesenolide	9.334	458.3051	C28 H42 O5
Camelledionol	16.321	440.3291	C29 H44 O3
Dihydrocapsaicin	4.241	307.2119	C18 H29 N O3

plaunotol	18.566	306.255	C20 H34 O2
Discadenine	4.336	304.1651	C14 H20 N6 O2
3-Ketosphinganine	14.256	299.2829	C18 H37 N O2
Bowdichione	9.913	298.0471	C16 H10 O6
N-Hexadecanoylpyrrolidine	18.508	309.302	C20 H39 N O
B6CH			
Amide C18	20.568	283.2867	C18 H37 N O
diisopropylethylamine	4.536	129.1516	C8 H19 N
4-Hexadecylmorpholine	22.495	311.3177	C20 H41 N O
Trihexylsilane	22.771	311.3177	C20 H41 N O
bis(4-Octylphenyl)amine	23.606	393.3385	C28 H43 N
Tetrabutylthiuram Disulfide	20.197	408.1749	C18 H36 N2 S4
Hexadecanamide	18.887	255.2556	C16 H33 N O
4-Hexadecylmorpholine	23.599	311.3177	C20 H41 N O
1-Heptadec-1-ynyl-cyclopentanol	18.762	320.3068	C22 H40 O
N-[(1E)-1-Cyano-1-propen-1-yl]formamide	7.312	110.0481	C5 H6 N2 O
2-Amino-4,5,6,7-tetrahydro-1-benzothiophene-3-carbonitrile	8.625	178.0561	C9 H10 N2 S
Safingol	13.503	301.2974	C18 H39 N O2
2-[(1,1-Dimethylethyl)sulfonyl]benzothiazole	11.78	255.0382	C11 H13 N O2 S2
4,7-dithien-2-yl-2,1,3-benzothiadiazole	16.618	299.9843	C14 H8 N2 S3
2-Mercaptobenzothiazole	10.875	166.9861	C7 H5 N S2
B30CH			
Amide C18	20.548	283.2866	C18 H37 N O
1-Heptadec-1-ynyl-cyclopentanol	22.527	311.3177	C22 H40 O
diisopropylethylamine	4.732	129.1516	C8 H19 N
4-Hexadecylmorpholine	22.812	311.3177	C20 H41 N O
Tetrabutylthiuram Disulfide	20.198	408.1747	C18 H36 N2 S4
bis(4-Octylphenyl)amine	23.672	393.3382	C28 H43 N
Safingol	13.496	301.2974	C18 H39 N O2
2-[(1,1-Dimethylethyl)sulfonyl]benzothiazole	11.784	255.0381	C11 H13 N O2 S2
2-Mercaptobenzothiazole	10.87	166.986	C7 H5 N S2
N,N-Dihexyldodecanamide	19.901	367.3803	C24 H49 N O
Amide C22	19.747	339.3491	C22 H45 N O
Ceramide Ng	22.982	567.5575	C36 H73 N O3
Erucamide	21.115	337.3334	C22 H43 N O
[1-methyl-2-(octadecylamino)-2-oxo-ethyl] acetate	20.057	383.3387	C23 H45 N O3
B200CH			
Urocanic Acid	0.966	138.0424	C6 H6 N2 O2
Methyl-3,4,6,10b-tetrahydropyrano[3,2-c]isochromene-4a,7,9(2H)-triol	14.178	252.1007	C13 H16 O5
3-hydroxy-10-methoxy-4,9-dimethyl-10-oxodeca-6,8-dienoic acid	15.218	148.0156	C8 H4 O3
trigonelline	0.889	137.0473	C7 H7 N O2
carnitine	0.842	161.1046	C7 H15 N O3
betaine	0.868	117.0786	C5 H11 N O2

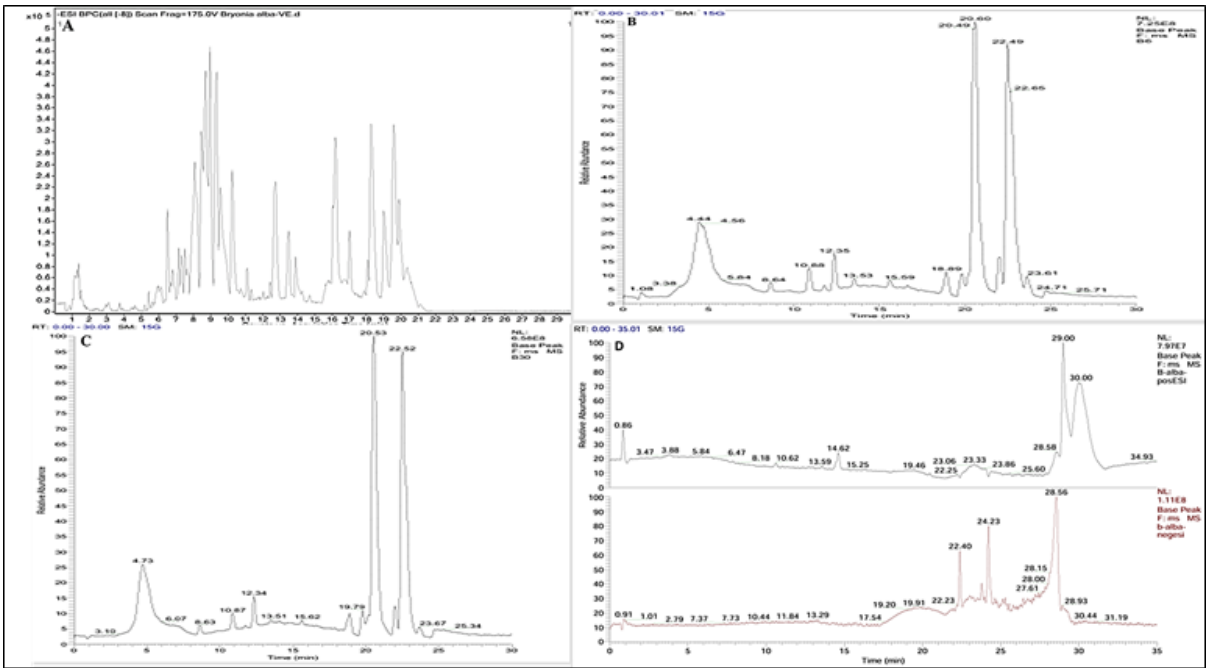

Figure 1. Chromatogram of A) BHMT B) B6CH C) B30CH D) B200CH

4.2 *In Silico* Study

Table no 2: Docking Score showing best results for all the proteins and components docked for Diclofenac A) BHMT B) B6CH C) B30CH D) B200CH

Protein / Ligand	Scores						
	3apc	3fmk	4xum	5ikr	5f1a	5oqw	7laf
Diclofenac (standard)	-20.01	-12.93	-9.2	-19.34	-22.8	-18.69	-23.5
A) *BHMT (5 ligand)*							
Discadenine	-22.53	-22.74	-16.75	-24.13	-26.52	-19.63	-23.73
Bowdichione	-19.64	-15.61	-15.88	-27.93	-24.02	-16.24	-27.63
Ganoderic Acid	-14.29	-14.73	2.39	-11.33	-8.38	-5.93	-10.66
Dihydrocapsaicin	-11.36	-8.13	-15.36	-14.68	-10.11	-6.56	-15.99
Cucurbitacins	-16.79	-10.81	0.14	-13.23	-12.35	-7.46	-17.26
B) *B6CH (4 ligand)*							
Proline	-32.5	-10.1	-18.1	-21.9	-20.8	-22.1	-22
2-[5-(2-Hydroxypropyl)Oxolan-2-YL]Propanoic Acid	-16.8	-11.2	-12.2	-25.9	-19.2	-17.2	-19.1
8-(4-Hydroxyphenyl)-3-Methoxy-6,7-Dimethyl-5,6,7,8-Tetrahydronaphthalen-2-Ol001	-15.1	-12.2	-12.6	-15	-17.3	-10.1	-24
-Hydroxy-7,8,14-Trimethoxy-17-Methyl-12,16,21-Trioxapentacyclo[15.3.1.02,15.04,13.06,11]Henicosa-2(15),3,6(11),7,9,13-Hexaen-5-One	-12.4	-9.4	-16.9	-16.5	-15.8	-13.7	-23.6
C) *B30CH (3ligands)*							
8,9-Dihydroxy-2,10,10-Trimethyltricyclo[6.3.0.01,5]Undec-6-Ene-6-Carboxylic Acid _001	-16.34	-10.88	-7.77	-14.78	-15.29	-19.40	-18.58
8-(4-Hydroxyphenyl)-3-Methoxy-6,7-Dimethyl-5,6,7,8-Tetrahydronaphthalen-2-Ol001	-14.64	-12.41	-7.35	-9.89	-17.27	-10.08	-12.77
[5-(2-Hydroxypropyl)Oxolan-2-YL]Propanoic Acid001	-13.89	-11.17	-5.73	-11.85	-13.86	-17.24	-19.43
D) *B200CH (6 Ligand)*							
Urocanic Acid	-18.53	-17.14	-17.62	-33.07	-22.34	-16.72	-24.26
Methyl-3,4,6,10b-Tetrahydropyrano[3,2-C]Isochromene-4a,7,9(2H)-Triol__001	-16.22	-12.45	-6.25	-20.07	-18.91	-12.65	-19.06
3-Hydroxy-10-Methoxy-4,9-Dimethyl-10-Oxodeca-6,8-Dienoic Acid001	-14.91	-19.06	-13.03	-29.75	-19.97	-14.50	-22.50
Trigonelline	-13.67	-15.89	-14.77	-20.73	-16.70	-15.33	-18.85
Carnitine	-12.26	-12.41	-5.58	-19.44	-16.22	-12.52	-16.44
Betaine	-11.09	-10.61	-9.88	-20.78	-12.44	-10.98	-14.11

Table no 3: Interaction Analysis through docking studies

3APC				
Compound	**Score (kcal/mol)**	**Interacting Amino Acid**	**Nature of Bond**	**Bond Distance (Å)**
Diclofenac	-20.01	Hid 169 Arg 476	H-Bond Salt-bridge	2.05 4.92
Discadenine	-22.53	Glu 302 Arg 277	H-Bond Salt-bridge	1.80 4.80
Bowdichione	-19.64	Glu 880	H-Bond	2.06
3FMK				
Diclofenac	-12.93	Lys 53 Trp18 Phe 90	H-Bond Pi-Pi stacking Pi-Pi stacking	1.93 5.35 5.10
Discadenine	-22.74	Ser 154 Asn 155 Asp 168	Aromatic Bond H-Bond H-Bond	1.54 1.68 2.41
Bowdichione	-15.61	Thr175 Glu178	H-Bond H-Bond	2.65 2.00
4XUM				
Diclofenac	-9.2	Glu 207 Asp 210	Aromatic Bond H-Bond	1.67 2.21
Discadenine	-16.75	Glu 295 Arg 288 Glu 295	Salt-bridge Salt-bridge H-Bond	3.51 2.95 1.79
Bowdichione	-15.88	Glu 295 Leu 228 Arg 288 Arg 288	Aromatic Bond H-Bond Pi-cation Pi-cation	2.61 1.74 2.95 2.93
5IKR				
Diclofenac	-19.34	Gly 225 Leu 224 Leu 224 Arg 376 Arg376	Aromatic Bond Aromatic Bond Aromatic Bond H-Bond H-Bond	2.77 2.56 2.36 2.16 1.62
Discadenine	-24.13	Pro 84 Lys 83 Glu 524 Phe 470	Aromatic Bond Salt-bridge H-Bond H-Bond	1.40 2.00 1.63 2.79
Bowdichione	-27.93	His 39 Arg 44 Arg 469 Lys 468 His 39	Aromatic Bond H-Bond H-Bond H-Bond H-Bond	2.52 1.92 2.30 2.25 2.25
5F1A				
Diclofenac	-22.8	Ser 126 Arg 44 Ile 124	Aromatic Bond Salt-bridge H-Bond	2.02 1.80 2.82
Discadenine	-26.52	Hid39 Cys41 Tyr130	H-Bond H-Bond Pi-Pi stacking	2.21 1.64 5.34
Bowdichione	-24.02	Cys 36	H-Bond	5.34
5OQW				
Diclofenac	-18.69	Glu 349	H-Bond	2.06
Discadenine	-19.63	Glu 349 Glu 349 Glu 318	Salt-bridge Salt-bridge H-Bond	4.19 4.68 1.55
Bowdichione	-16.24	Hid 346	Aromatic Bond	2.43
7LAF				

Diclofenac	-23.5	Leu172 Lys 175 Arg618	Aromatic Bond Aromatic Bond Salt-Bridge	1.98 2.10 2.48
Discadenine	-23.73	Asp 625 Asp 625	Salt-bridge H-Bond	2.90 1.90
Bowdichione	-27.63	Glu 141 Glu 105 Glu 108 Glu 119	Aromatic Bond Aromatic Bond Aromatic Bond H-Bond	2.73 2.44 2.48 1.63

After describing the statistical approach, we next summarize the results of the virtual screening. In total, 48 ligands were virtually tested against seven protein targets (PDB IDs: 3APC, 3FMK, 4XUM, 5F1A, 5IKR, 5OQW, and 7LAF) after being identified by HR-LCMS analysis of BHMT and its dilutions (B6CH, B30CH, and B200CH). Eighteen of these ligands were able to dock with the chosen targets. The most positive findings were notably shown by Discadenine and Bowdichione, which showed excellent binding affinities and interactions with all target proteins. According to Tables 2 and 3, their docking scores were on par with or better than those of the reference chemical, diclofenac. Conversely, as shown by their comparatively low docking scores, the other ligands showed either weak or insignificant interactions with the targets. Figures through 3D structural representations of protein–ligand interactions.

For the 3APC (TNF-alpha) protein, energy score of -20.01 kcal/mol, diclofenac demonstrated strong bounding interactions with the target. Discadenine (−22.53 kcal/mol) exhibited stronger binding affinity than Diclofenac, as shown by its more negative docking score, while Bowdichione (−19.64 kcal/mol) demonstrated a similar, though slightly weaker, affinity compared to Diclofenac. All three ligands—Diclofenac, Discadenine, and Bowdichione—showed significant hydrogen-Bond interactions with His169, Glu302, and Glu880. Additionally, Arg476 and Arg227 formed salt-bridge interactions with both Discadenine and Diclofenac, supporting their higher target engagement.

Discadenine had the greatest binding among the ligands evaluated for the 3FMK (TNF-alpha) protein, energy score of −22.74 kcal/mol, were as Bowdichione with −15.61 kcal/mol. Both compounds surpassed the reference ligand Diclofenac, which scored −12.93 kcal/mol, in terms of binding affinity. All three ligands demonstrated consistent hydrogen Bond interactions with the essential residues Lys53, Asn155, Asp168, Thr175, and Glu178, while only Diclofenac displayed enhanced binding stability through π–π stacking with Trp18 and Phe90.

4XUM (Cox-2): For the 4XUM protein target, the selected ligands demonstrated binding affinities that were either equal to or greater than those of the reference ligand Diclofenac; the docking scores were −9.2 kcal/mol for Diclofenac, −15.88 kcal/mol for Bowdichione, and −16.75 kcal/mol for Discadenine, indicating a better predicted contact for both natural ligands. Structural analysis showed aromatic interactions between Diclofenac and Glu207 at a distance of 1.67 Å, and between Bowdichione and Glu295 at a distance of 2.61 Å. Discadenine formed salt-bridge interactions with Glu295 and Arg288 at distances of 3.51 Å and 2.95 Å, respectively, and π–cation interactions involving Arg288 at 2.95 Å and 2.93 Å, further confirming the ligand's strong binding stability.

5IKR (Cox-2): Discadenine and Bowdichione formed π–π stacking contacts with Pro84 (1.40 Å) and His39 (2.52 Å), respectively, according to molecular docking research. By contrast, Gly225 (2.77 Å) and Leu224 (2.56 Å, 2.36 Å) showed aromatic (π–π) interactions with the reference ligand Diclofenac. Diclofenac created H-Bonds with Arg376, Glu524, and Phe470, according to hydrogen Bonding analysis, whereas Dicadenine interacted with Arg44, Arg469, and Lys468 through H-Bonds. Bowdichione and His39 showed a crucial H-Bond interaction.

5F1A (Cox-1): Both Discadenine and Bowdichione demonstrated binding affinities similar to the reference ligand (Diclofenac, −22.8 kcal/mol) in the docking investigation against the 5F1A protein structure, with docking scores of −26.52 kcal/mol and −24.02 kcal/mol, respectively. At a distance of 5.34 Å, Discadenine produced a π–π stacking interaction with Tyr130 in addition to forming hydrogen Bond interactions with residues His39, Cys41, and Cys36. The reference ligand demonstrated an aromatic interaction with Ser126 (Bond distance 2.02 Å) and hydrogen Bonding with Ile124 (Bond length 1.80 Å). Additionally, at 2.82 Å, a salt bridge between Diclofenac and Arg44 was detected. These interactions show that the test ligands have a stable binding conformation within the active site and have an affinity that is either equal to or greater than that of the reference molecule.

TNF-alpha (5OQW): The binding affinity is -19.63 kcal/mol, Discadenine outperforms the reference ligand, Diclofenac, which had an affinity of -18.69 kcal/mol. Bowdichione formed an aromatic interaction with His346 and showed a substantially lesser affinity (−16.24 kcal/mol). Glu349 and the reference ligand, diclofenac, created a hydrogen Bond. Furthermore, Discadenine formed salt bridge connections with Glu349 at 4.19 Å and 4.68 Å, respectively, and demonstrated a hydrogen Bond interaction with Glu318 (Bond distance: 1.55 Å).

7LAF (15-lipoxygenase-2): In comparison to the reference ligand Diclofenac (−23.5 kcal/mol), Bowdichione showed the highest binding affinity (−27.63 kcal/mol), while Discadenine possessed interaction

strength of −23.73 kcal/mol. Leu172 and Lys175 created π–π stacking contacts with Diclofenac, whereas Glu141, Glu105, and Glu108 formed numerous aromatic connections with Bowdichione. Diclofenac and Discadenine both demonstrated improved ligand–protein stability by forming salt-bridge interactions with important active-site residues.

In brief, both Discadenine and Bowdichione consistently demonstrated higher binding affinities than the reference ligand Diclofenac, as determined by molecular docking across various protein targets (PDB IDs: 3APC, 3FMK, 4XUM, 5IKR, 5F1A, 5OQW, and 7LAF). Discadenine showed particularly favorable scores (up to −26.52 kcal/mol), while Bowdichione showed the highest affinity (−27.93 kcal/mol) at 5 IKR. Both ligands demonstrated improved binding stability and specificity by forming a variety of stabilizing interactions with important active-site residues, including as H-Bonds, π–π stacking, salt-bridges, and aromatic interactions. According to these findings, Discadenine and Bowdichione have a high potential for use as bioactive substances because their binding energies and interaction profiles are on equal to or better than those of the common medication diclofenac.

4.3. Dynamic study analysis

The constancy of the ligand-protein combination in its bound form is assessed using molecular dynamics simulations. In addition to Bowdicione, Descadinine, and the common reference Diclofenac, other protein-ligand complexes (3APC, 3FMK, 4XUM, 5IKR, 5OQW, 5F1A, and 7LAF) were investigated. The results of the MD simulation were examined in order to comprehend the ligand -protein pathways throughout simulation and find limitations on the target. RMSD, RMSF, SASA, potential energy, and ligand gyration were all included in the investigation. Below (fig. no. 9-20) is an explanation of each MD simulation component (43).

Comparative Performance of Compounds Across Different Proteins Across all simulated systems, the performance of ligands depends on: protein structural stability (SSE, RMSD), ligand stability (RMSD, RMSF), and binding interactions (ionic, H-Bond, hydrophobic). Among the selected proteins, some specific proteins showed the best ligand performance, which was observed for 3APC, 5IKR, 5OQW, 5F1A, and 7LAF. Diclofenac, considered a standard compound, displayed strong ionic interactions and good stability with almost all of the selective proteins. Bowdichione exhibited good ionic interactions, stable binding pocket interactions (ionic, H-Bond, hydrophobic), and ligand stability (RMSD, RMSF) compared to the standard Diclofenac. Lower flexibility (Bowdichione) favors stable binding, whereas excessive flexibility (Discadenine) may reduce binding consistency.

Overall, it was noted that in selective proteins, when assessing the structural permanency of the ligand – protein complex over time, an important parameter RMSD. Protein RMSD: A steady trajectory within ~1-3 Å shows that the protein's structural integrity is maintained throughout the simulation. Ligand RMSD: Higher deviations signify potential diffusion away from the binding pocket, while lower and stable values imply whether the ligand is still securely attached to the active site. RMSF sheds light on how flexible each amino acid sequence is. Terminal sections and loop segments usually exhibit higher volatility. Stable ligand-protein interactions are indicated by reduced fluctuations at the binding site. Stable binding was confirmed by the observation that all systems displayed anticipated fluctuation patterns with little variation in the active site region.

RMSD, RMSF, and secondary structure analysis verified that The target protein and all three ligands generated stable complexes. over the course of the 100 ns simulation. Among them, diclofenac showed the strongest binding interactions, validating the simulation approach. Importantly, the natural compound Bowdichione demonstrated comparable stability and interaction characteristics, highlighting its potential as a promising anti-inflammatory lead molecule. In contrast, discadenine exhibited higher flexibility, which may compromise binding stability despite favorable interaction potential. Ligand performance is protein-dependent, according to a comparative molecular dynamics study across several protein systems. Because of ionic interactions, diclofenac consistently showed great binding affinity, while Bowdichione showed superior structural stability and consistent binding across a variety of proteins, including big and complex systems like 7LAF. Interestingly, Bowdichione performed as well as or better than diclofenac in a number of systems (3APC, 5OQW, and 7LAF), indicating that it may be a promising lead compound.

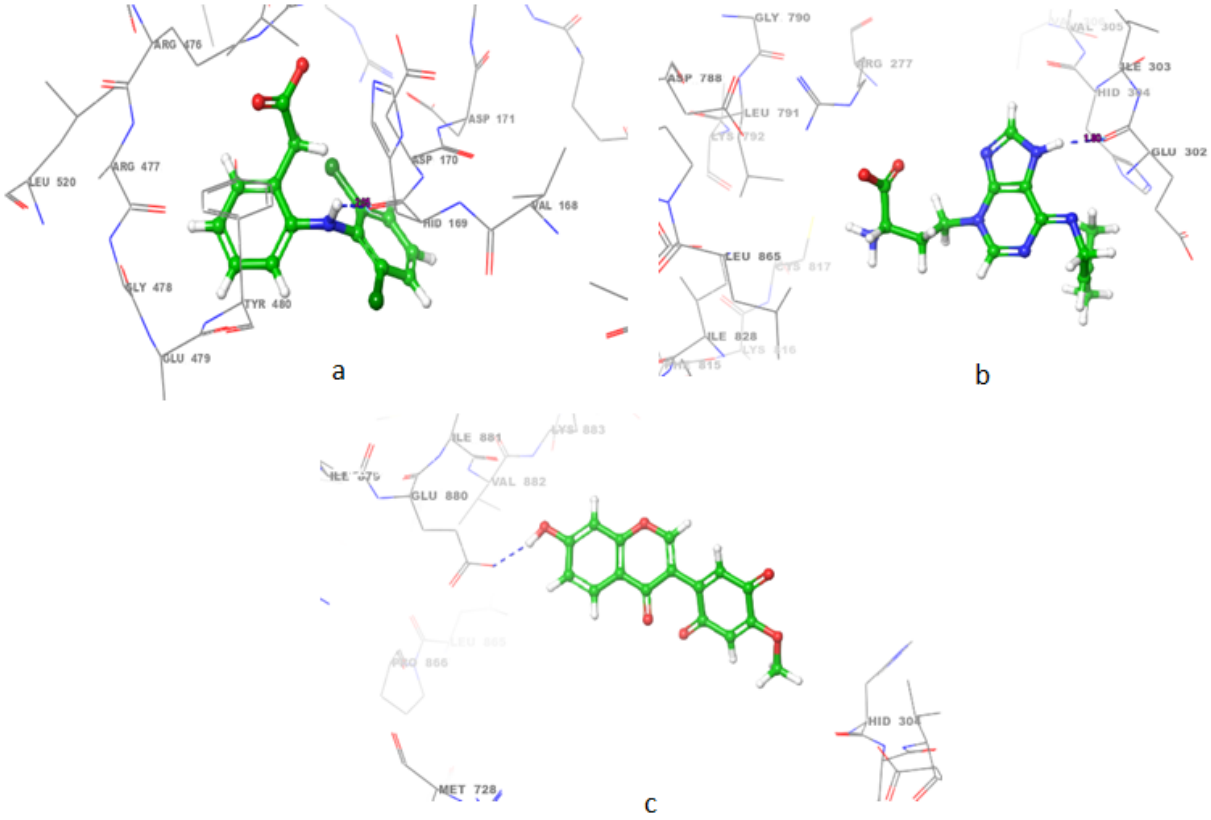

Figure 2: Docking Interactions for 3APC protein with a) Diclofenac (reference ligand), b) Discadenine, c) Bowdichione

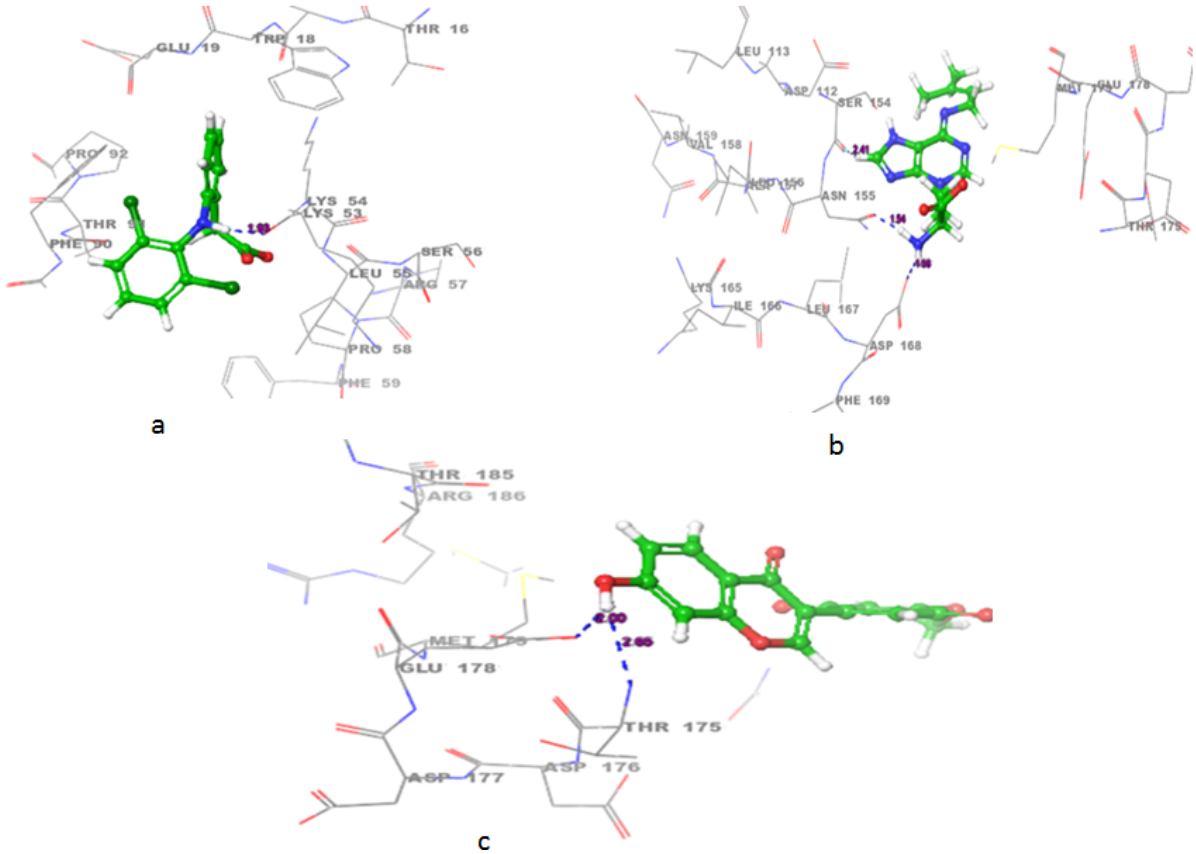

Figure 3: Docking Interactions for 3FMK protein with a) Diclofenac (reference ligand), b) Discadenine, c) Bowdichione

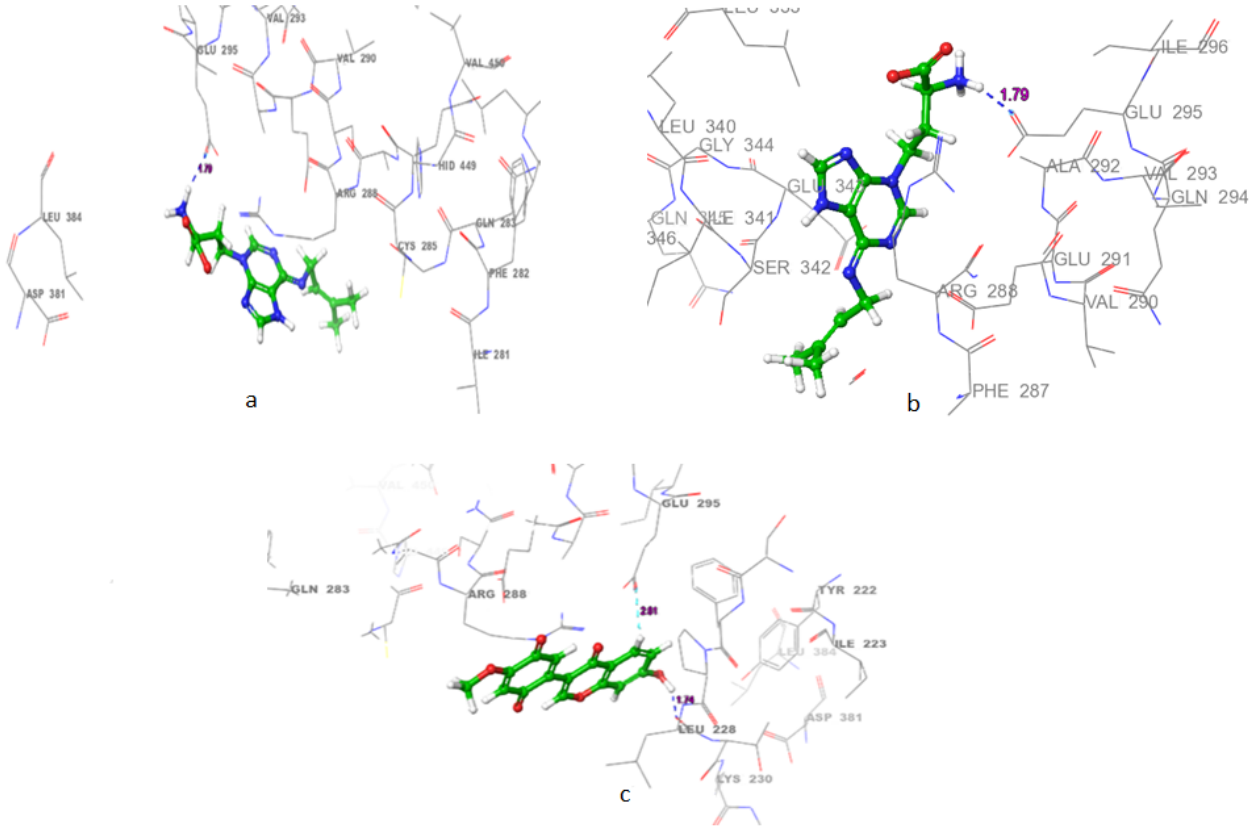

Figure 4: Docking Interactions for 4XUM protein with a) Diclofenac (reference ligand), b) Discadenine, c) Bowdichione

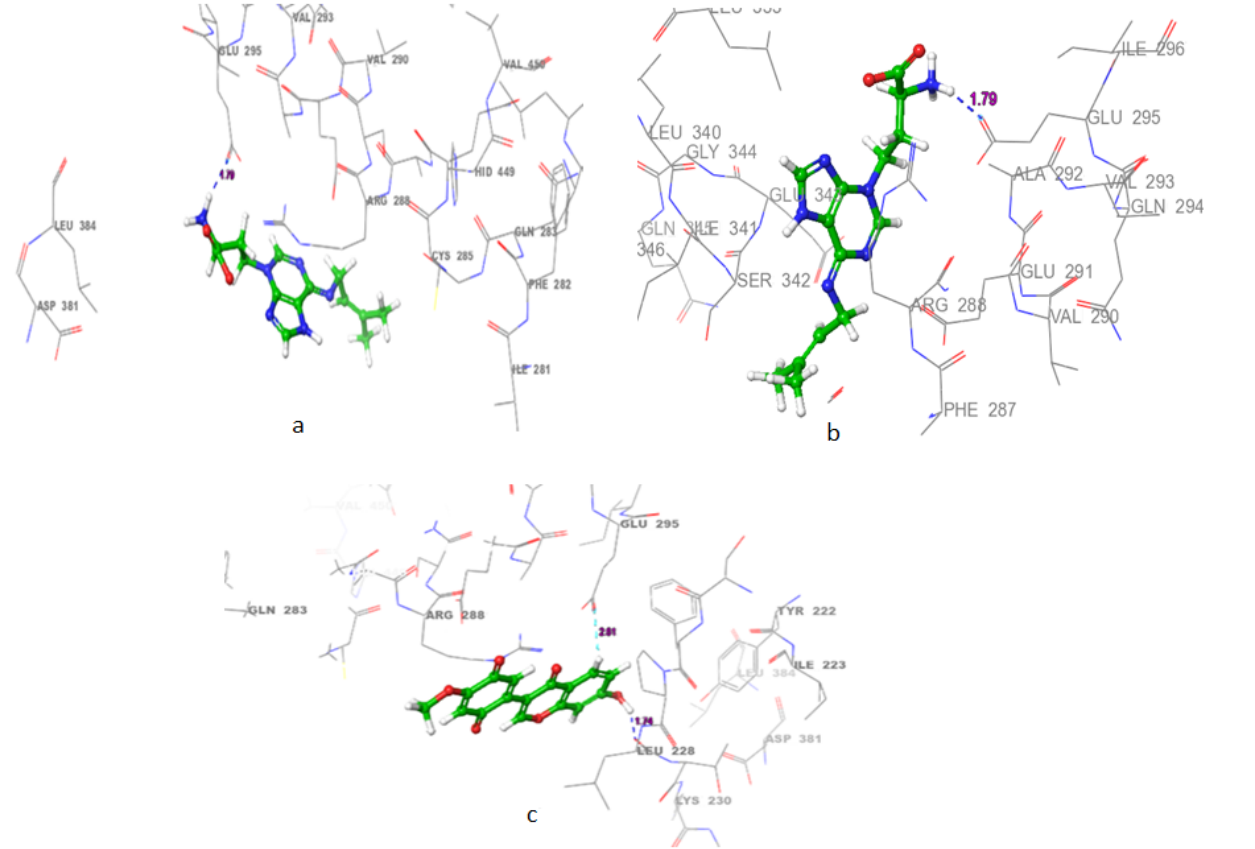

Figure 5 : Docking Interactions for 5IKR protein with a) Diclofenac (reference ligand), b) Discadenine, c) Bowdichione

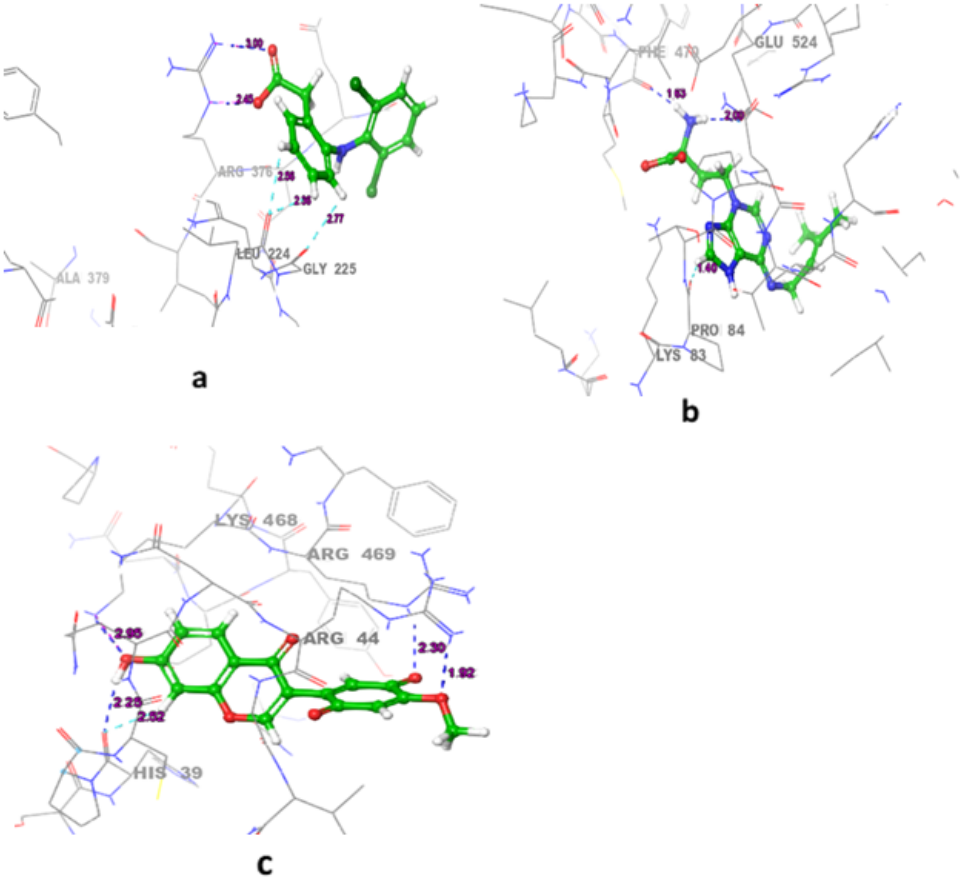

Figure 6: Docking Interactions for 5F1A protein with a) Diclofenac (reference ligand), b) Discadenine, c) Bowdichione

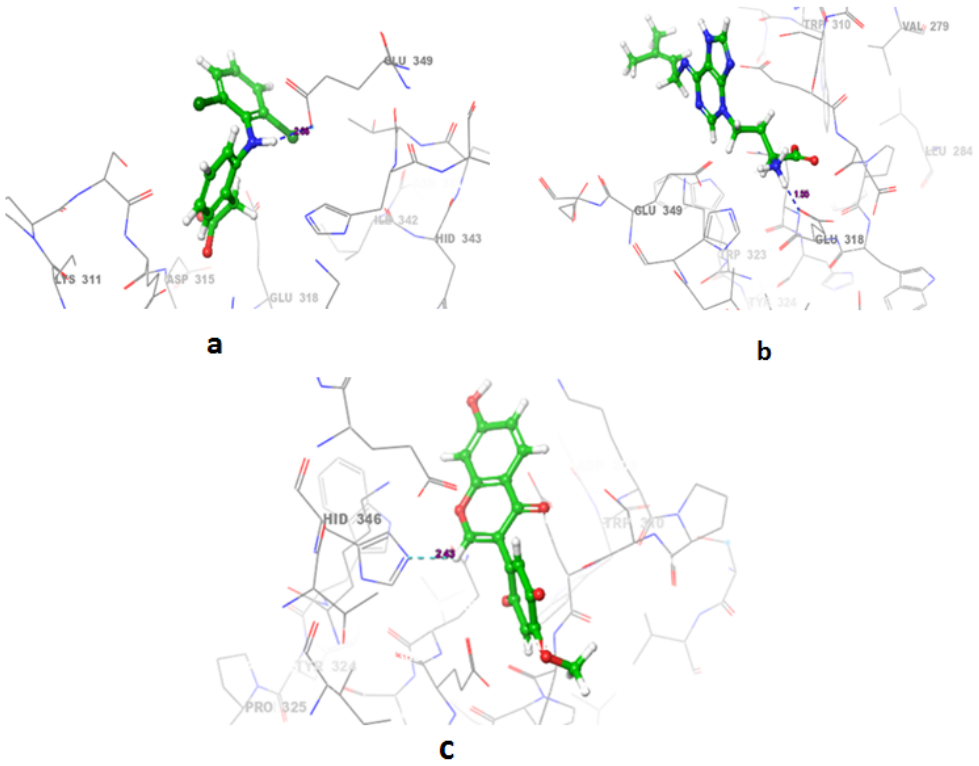

Figure 7: Docking Interactions for 5OQW protein with a) Diclofenac (reference ligand), b) Discadenine, c) Bowdichione

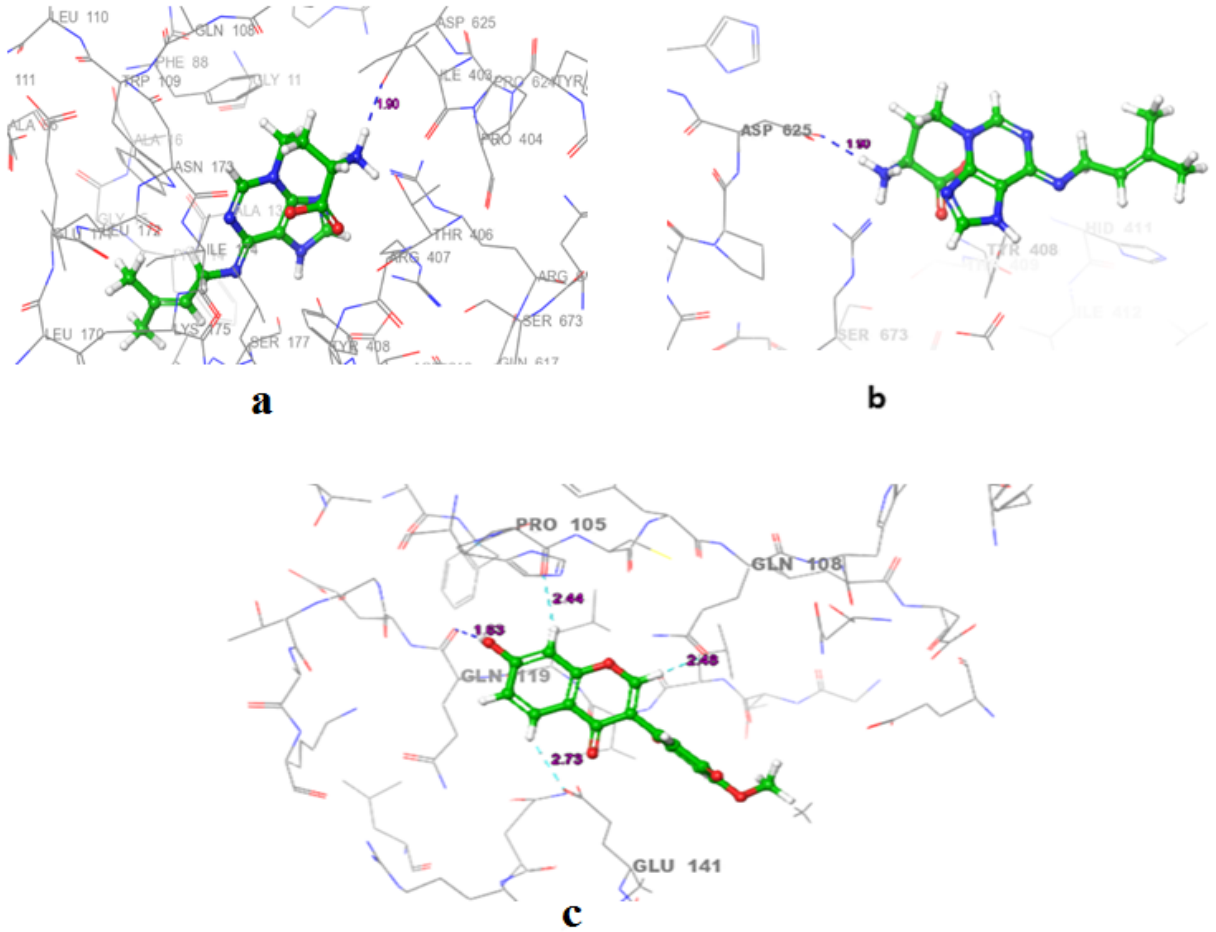

Figure 8: Docking Interactions for 7LAF protein with a) Diclofenac (reference ligand), b) Discadenine, c) Bowdichione

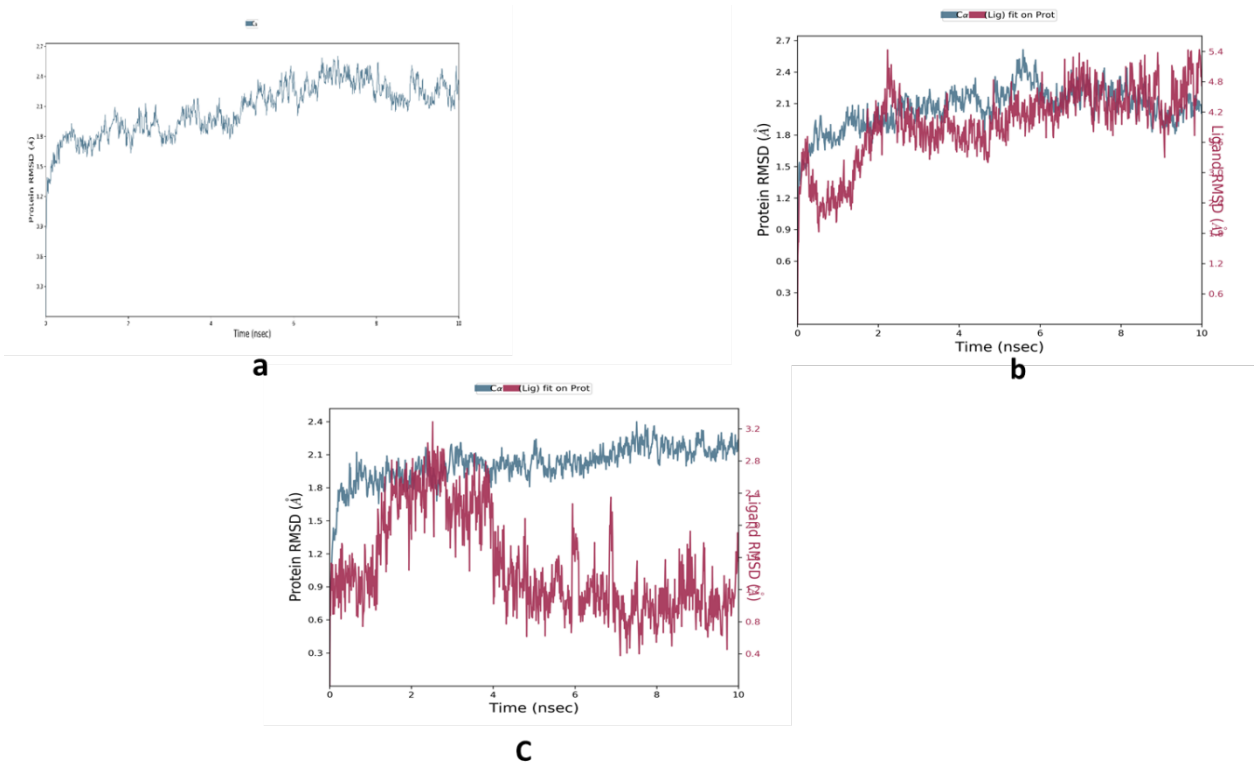

Figure 9: RMSD for 3APC protein with a) Diclofenac (reference ligand), b) Discadenine, c) Bowdichione

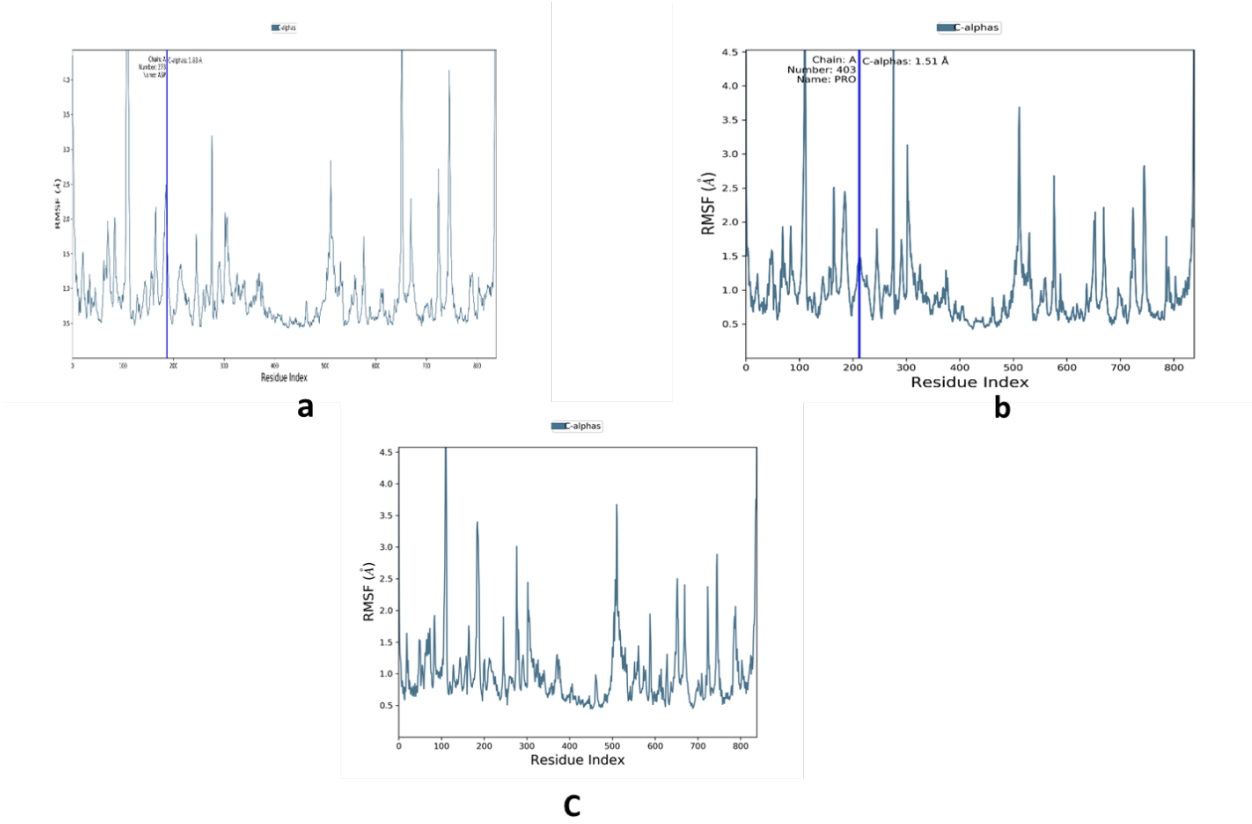

Figure 10: RMSF for 3APC protein with a) Diclofenac (reference ligand), b) Discadenine, c) Bowdichione

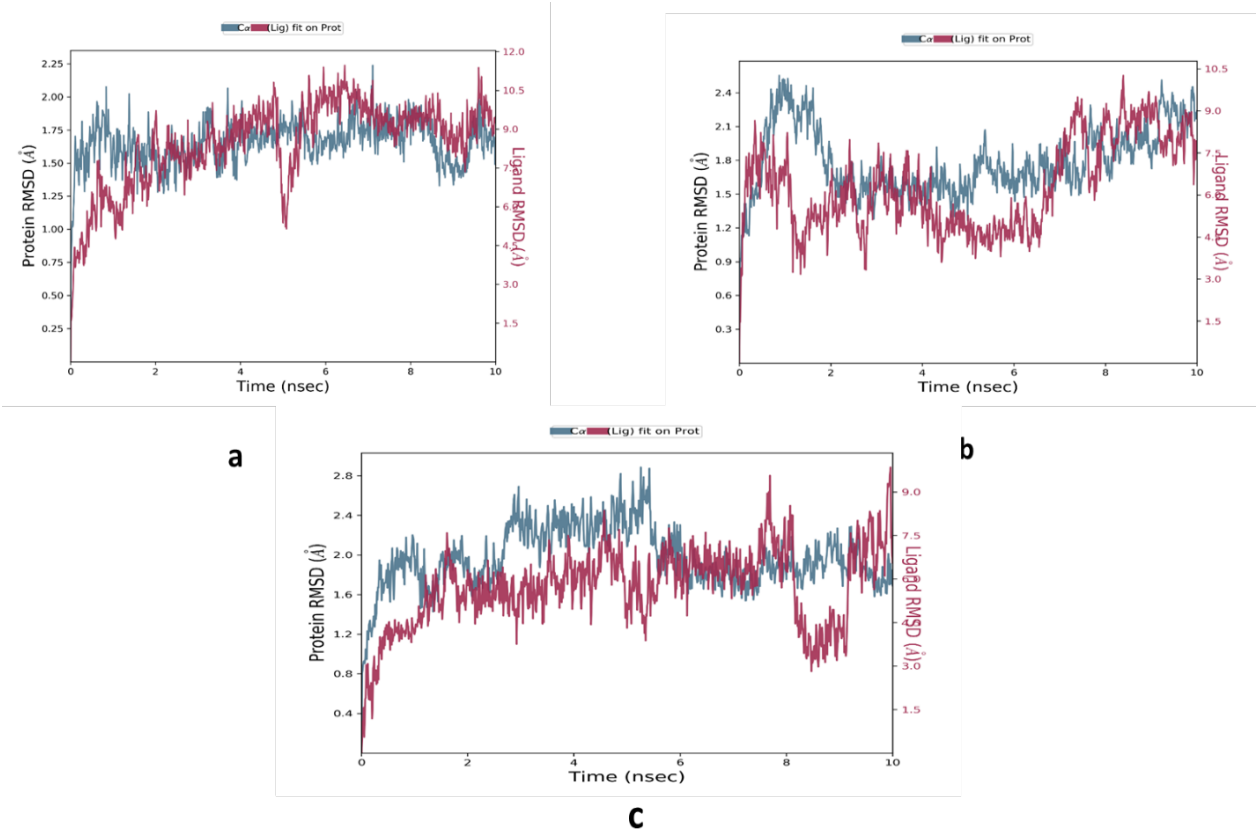

Figure 11: RMSD for 5OQW protein with a) Diclofenac (reference ligand), b) Discadenine, c) Bowdichione

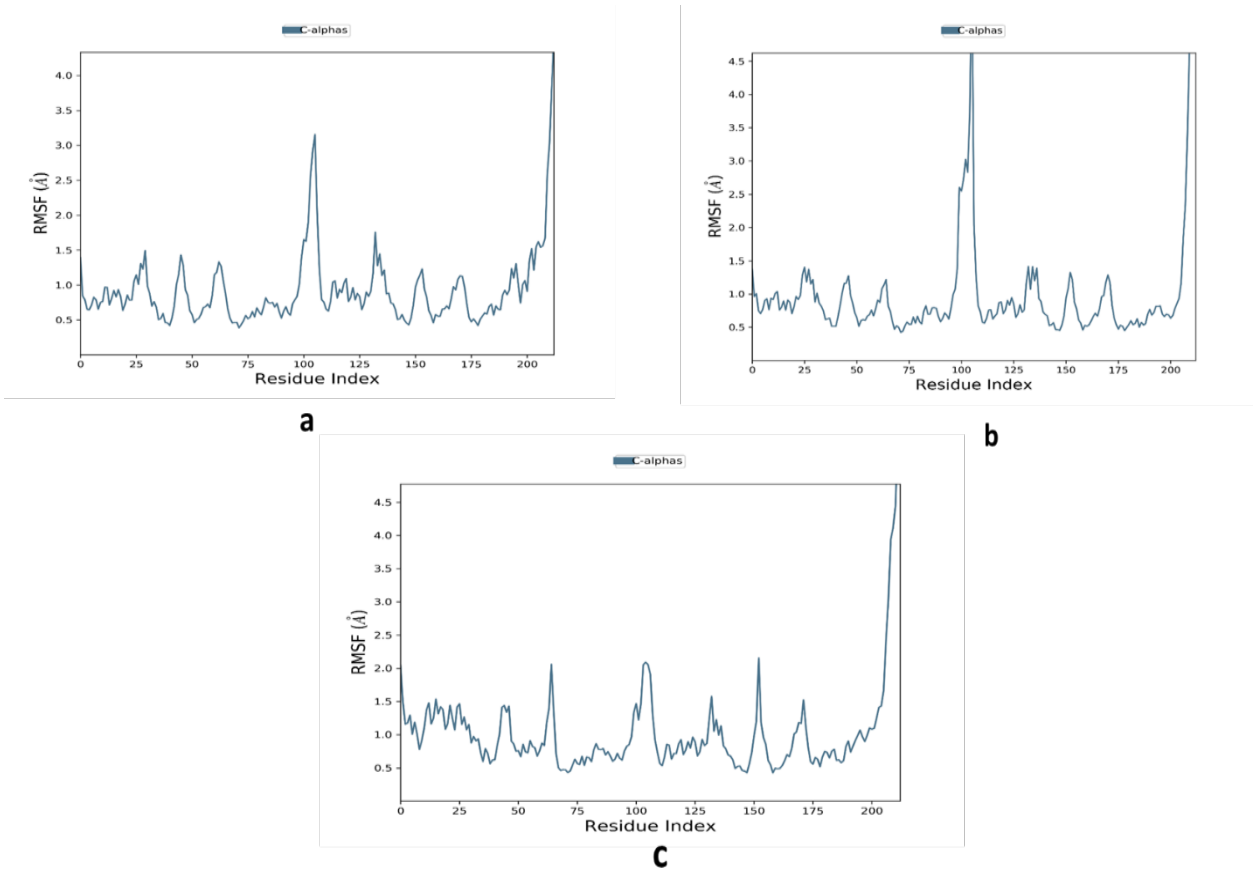

Figure 12: RMSF for 5OQW protein with a) Diclofenac (reference ligand), b) Discadenine, c) Bowdichione

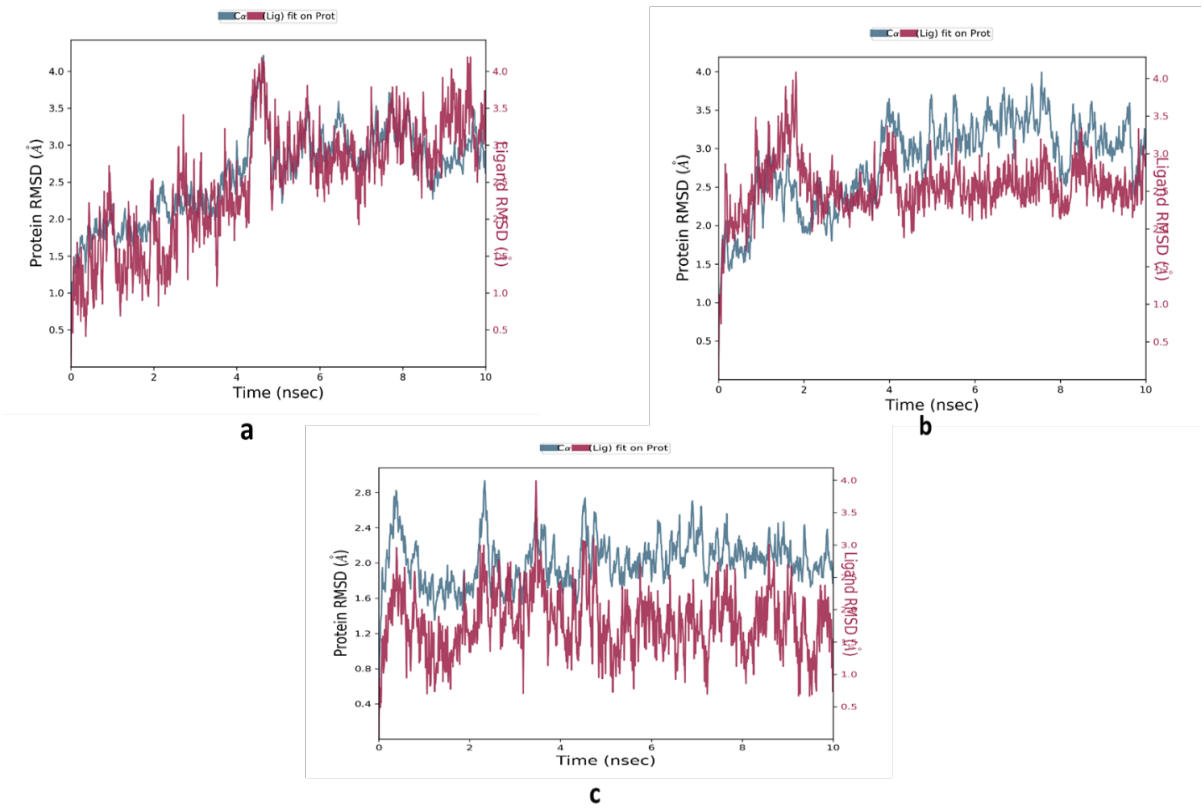

Figure 13: RMSD for 7LAF protein with a) Diclofenac (reference ligand), b) Discadenine, c) Bowdichione

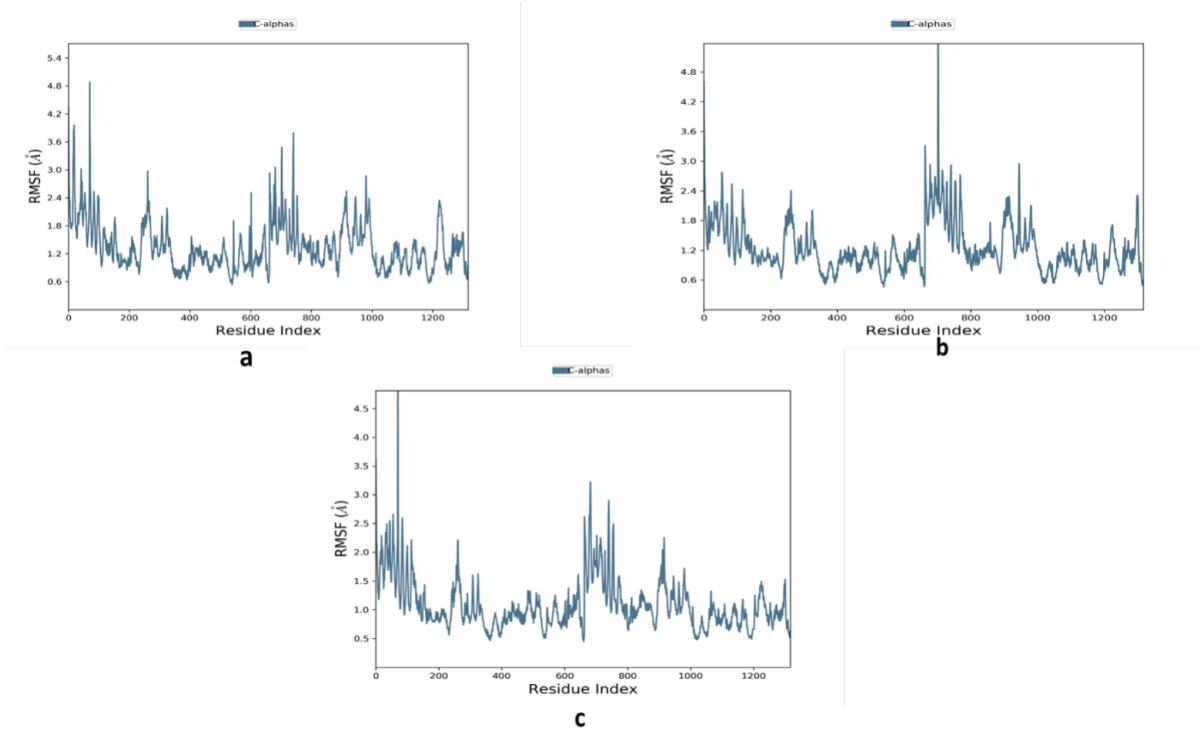

Figure 14: RMSF for 7LAF protein with a) Diclofenac (reference ligand), b) Discadenine, c) Bowdichione

Table no 4: SwissADME for the selected compounds:

Molecule	Molecular Weight (g/mol)	Rotating Bonds	H-Bond holders	H-Bond providers	Molar Refractivity	Ilogp	Xlogp3	GI absorption	Lipinski violations	Bioavailability score
Diclofenac	296.15	4	2	2	77.55	1.98	4.4	High	0	0.85
Discadenine	304.16	6	5	3	0	-0.966	-1.8	High	0	0.99
Bowdichione	298.05	2	6	1	77.53	1.66	1.12	High	0	0.56

Molecule	Chemical structure	Radar for Bioavaibility
Diclofenac	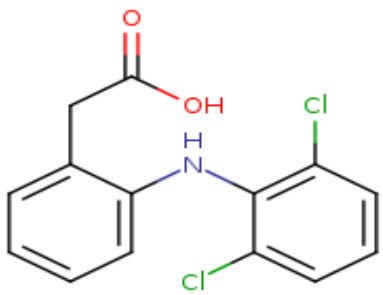	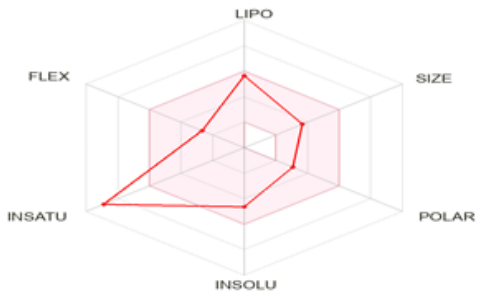
Discadenine	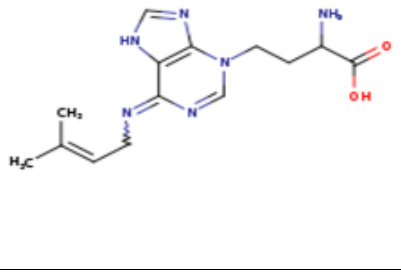	

Bowdichione	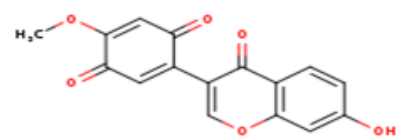	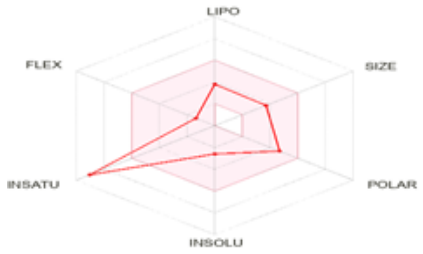

Figure 15: Chemical structures and bioavailability radar

Table no. 5: ADMET Prediction by ADMETlab 2.0

Compounds	BBB	HIA	PGP	CYP2C9 Inhibitor	CYP2D6 Inhibitor	CYP3A4 Inhibitor	Ames Toxicity	Carcinogenicity	Hepatotoxicity	AOT Class
Diclofenac	Yes	Yes	No	Yes	Yes	No	Yes	No	Yes	IV
Discadenine	Yes	Yes	No	Yes	No	No	Yes	No	Yes	III
Bowdichione	Yes	Yes	No	Yes	No	No	Yes	No	No	III

Note: AOT: Acute oral toxicity: I -0.774,II- 0.462-0.6238, III-0.7012,IV- 0.5275.

4.4 ADMET analysis:

SwissADME and ADMETlab 2.0 were used to evaluate absorption, distribution, metabolism, excretion, and toxicity. SwissADME was helpful in finding gastrointestinal absorption, bioavailability, and violations of the Lipinski rule for several chemicals, including Diclofenac, Discadenine, and Bowdichione, which were all followed by the molecules. (Table no. 4). The pharmacokinetic and toxicity profiles of diclofenac, discadenine, and bowdichione were assessed using in silico ADMET analysis. All three substances demonstrated high penetration of the blood-brain barrier (BBB) and human gastrointestinal absorption (HIA), indicating possible exposure to a central nervous system (CNS) and good systemic bioavailability. The likelihood of efflux-mediated drug resistance is minimal, as none of the drugs were identified as P-glycoprotein (PGP) substrates.

Discadenine and Bowdichione predicted to inhibit CYP2C9 in a selective manner. Inhibitory activity against CYP2C9 and CYP2D6 was shown by diclofenac. None of the compounds inhibited CYP3A4, indicating little chance of CYP3A4-mediated drug–drug interactions. According to toxicity predictions, all three ligands were Ames positive, suggesting that they might be mutagenic. Bowdichione showed no hepatotoxicity risk, but diclofenac and Discadenine were predicted to be hepatotoxic. Discadenine and Bowdichione were classified as class III, indicating moderate acute toxicity, while Diclofenac was placed in class IV according to the AOT classification. Discadenine and Bowdichione showed enhanced pharmacokinetic properties and not as much of anticipated hepatotoxicity when compared with diclofenac (Table no 5). ADMET was used to analyze promising pharmacokinetic features. A possible mutagenesis risk was revealed by positively predicted Ames compounds, underscoring the necessity for additional in vitro and in vivo toxicity testing.

4.5 *In Vivo* study analysis:

Wistar rats were given CFA to induce arthritis in order to evaluate anti-arthritic qualities of Bryonia alba mother tincture (BHMT) and its homeopathic dilutions (6C, 30C, and 200C). Animals treated with BHMT, particularly at concentrated and higher potencies (30C and 200C), maintained or grew body mass, equivalent to the normal control group, but animals in the illness control group steadily lost body weight over the course of the trial. Whereas CFA injection caused a large amount of paw edema on day 0 that continued in the disease control group, according to paw volume analysis using a plethysmometer. Rats given BHMT formulations, on the other hand, demonstrated a noticeable improvement in paw inflammation on days 14 and 21 after a progressive decrease starting on day 7. The BHMT 30C and 200C groups' decrease in paw edema by day 28 was similar with the standard group's reduction from diclofenac. After therapy, radiological tests were conducted and blood samples were taken for biochemical analysis. Following the animals' sacrifice, paw tissue homogenates were examined for inflammatory and oxidative stress indicators. The results demonstrated that substantial increases in BHMT potency significantly reduced lipid peroxidation (MDA levels), enhanced antioxidant enzyme activities (SOD, CAT, GST, and GSH), (Table 7; Fig. 16) and decreased serum levels of pro-inflammatory cytokines (TNF-α and IL-6) (Table 8; Fig. 17). These changes were comparable to those observed in the diclofenac-treated group. Although to a much lesser extent than at higher dosages, median potency (30C) still demonstrated substantial anti-inflammatory and antioxidant benefits.

Table 6. Effects of Homeopathic formulations on Paw volume at various days in Wistar rats with CFA Induced Inflammation

Sr No.	Groups	Paw volume at Various days (ml) (Mean ±SEM)				
		Day 0	Day 7	Day 14	Day 21	Day 28
1	Normal Control	1.03±0.05	1.04±0.05	1.07±0.05	1.04±0.03	1.04±0.03
2	Negative Control	1.03±0.05	1.32±0.16$^{\#\#}$	1.63±0.22$^{\#\#\#}$	2.31±0.28$^{\#\#\#}$	2.85±0.35$^{\#\#\#}$
3	Standard **(Diclofenac)**	1.01±0.04	1.07±0.09*	1.06±0.11**	1.04±0.04***	1.04±0.04***
4	BHMT	1.02±0.10	1.16±0.16	1.36±0.37	1.56±0.38*	1.52±0.34**
5	BHMT 6C	1.03±0.05	1.30±0.17	1.43±0.26	1.74±0.50*	2.03±0.75*
6	BHMT 30C	1.07±0.09	1.21±0.23	1.32±0.30	1.35±0.48**	1.47±0.85***
7	BHMT 200C	1.07±0.08	1.17±0.17	1.35±0.30	1.41±0.50*	1.40±0.63***
Data was analyzed by two-way ANOVA followed by Benferroni post hoc analysis. $^{\#\#\#}$p<0.001 compared to normal control group, * p<0.05, **p<0.01, ***p<0.001 compared to negative control (disease control)						

Table 7. Effects of Homeopathic formulations on serum for antioxidants parameter in Wistar rats with CFA Induced Inflammation

Groups	Oxidative stress parameters (antioxidants and MDA) on last day (Mean±SEM)			
	SOD (U/mg protein)	GSH mM/gm Tissue	Catalase (U/mg protein)	MDA formation (nmol/mg protein)
Normal Control	26.97±4.68	0.42±0.12	4.18±0.86	2.85±0.56
Disease Control	12.77±0.81$^{\#\#}$	0.10±0.04$^{\#\#}$	0.88±0.18$^{\#\#\#}$	13.15±2.91$^{\#\#\#}$
Standard (Diclofenac)	19.53±4.18*	0.21±0.07*	2.14±0.69***	5.22±1.70***
BHMT	24.90±4.19***	0.25±0.07***	2.84±1.31***	5.54±1.15**
BHMT 6C	19.62±2.77	0.47±0.62***	2.07±0.93***	6.99±1.64**
BHMT 30C	18.60±1.57***	0.23±0.07***	2.15±0.77***	5.90±1.60***
BHMT 200C	20.89±1.08***	0.21±0.02**	2.55±0.39***	4.77±1.59***
Data was analyzed by one-way ANOVA followed by Bonferroni post hoc analysis. $^{\#\#\#}$p<0.001 compared to normal control group, * p<0.05, **p<0.01, ***p<0.001 compared to negative control (disease control)				

Table 8. Effects of Homeopathic formulations on serum TNF-α Levels and IL-6 in Wistar rats with CFA Induced Inflammation

Sr No.	Groups	TNF-α pg/ml (Mean±SEM)	IL-6 pg/ml (Mean±SEM)
1	Normal Control	28.95±7.52	222.21±40.89
2	Disease Control	607.58±122.57$^{\#\#\#}$	915.15±114.03$^{\#\#\#}$
3	Standard (Diclofenac)	168.63±74.85***	422.30±159.23***
5	BHMT	484.63±105.31*	561.75±139.93**
10	BHMT 6C	306.46±74.40*	377.13±75.41***
11	BHMT 30C	205.04±72.04***	311.58±35.78***
12	BHMT 200C	215.27±44.90***	275.05±36.23***
Data was analyzed by one-way ANOVA followed by Bonferroni post hoc analysis. $^{\#\#\#}$p<0.001 compared to normal control group, * p<0.05, **p<0.01, ***p<0.001 compared to negative control (disease control).			

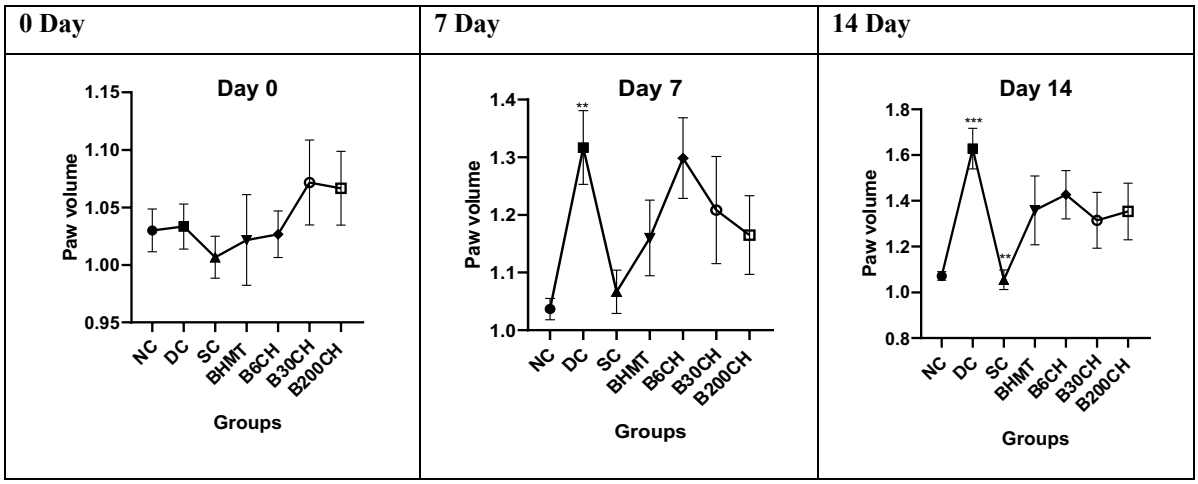

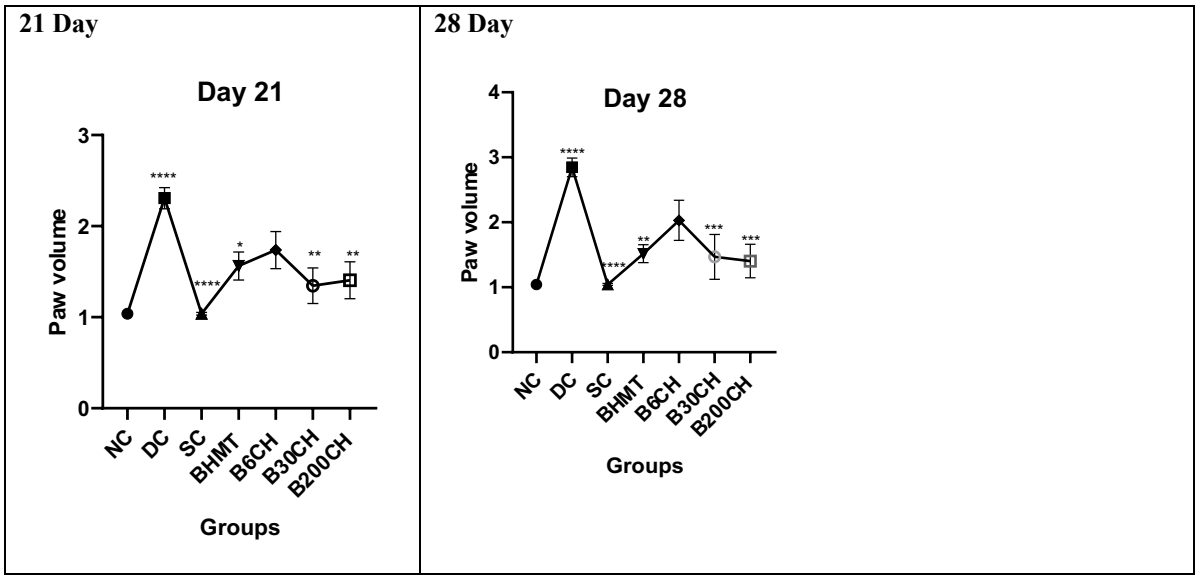

Figure 16: Paw volume Graphical representation for Wistar rats with CFA induced-arthritis at 0, 7,14,21,28 days.

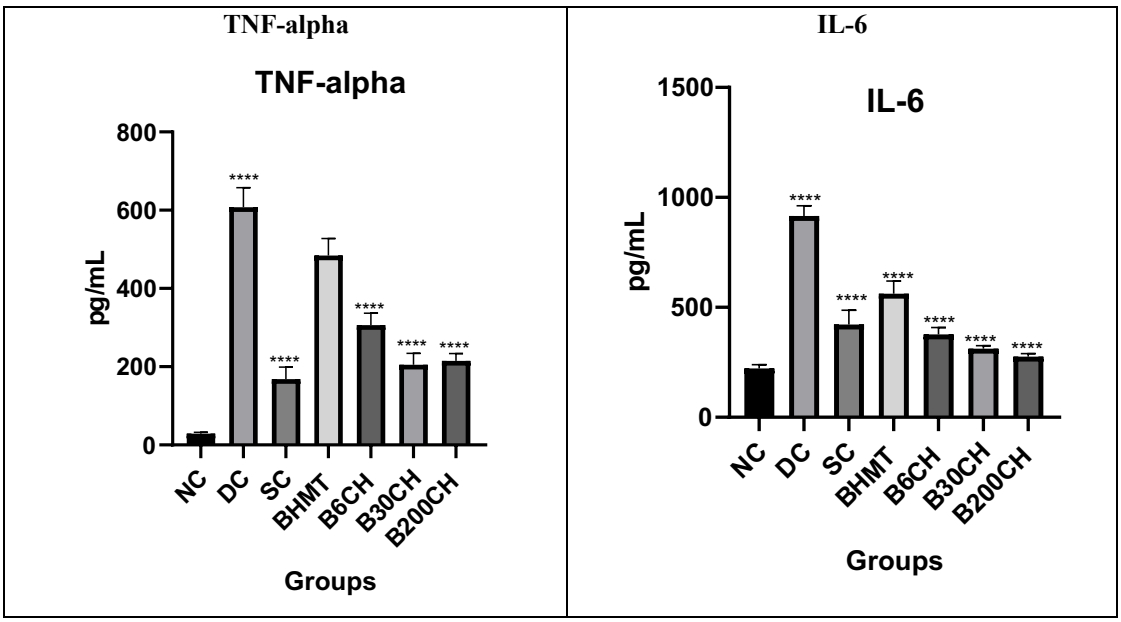

Figure .17: Graphical representation for TNF-alpha, IL-6 in Wistar rats with CFA induced –Arthritis

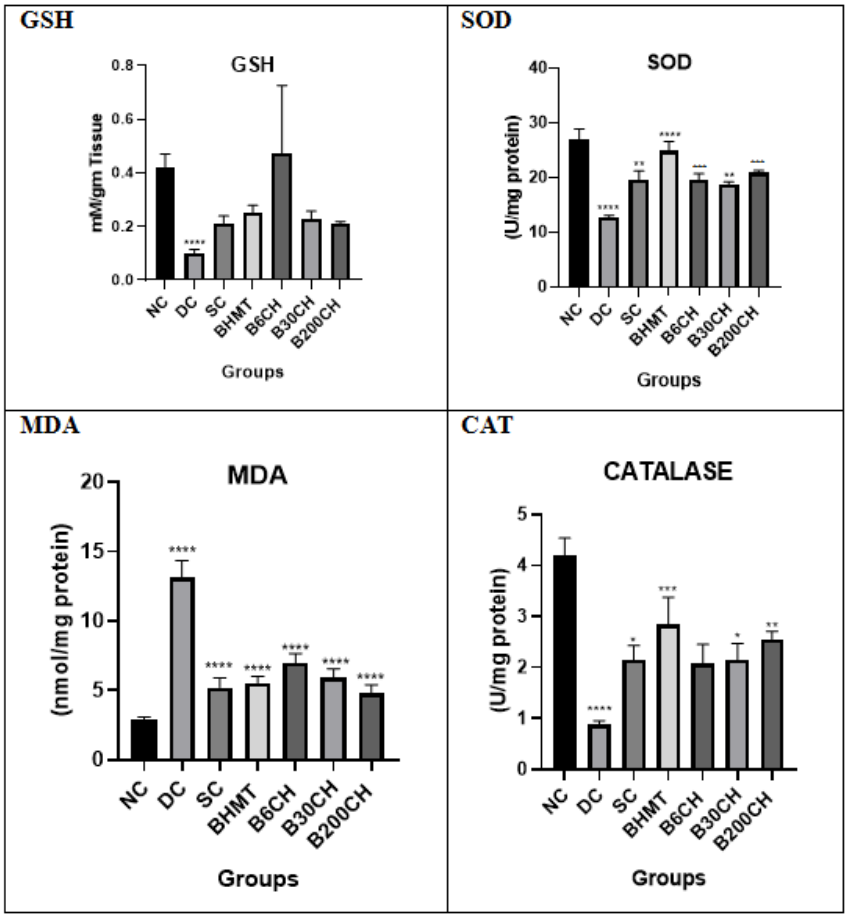

Figure 18: Graphical representation for oxidative stress parameters in Wistar rats with CFA induced –Arthritis

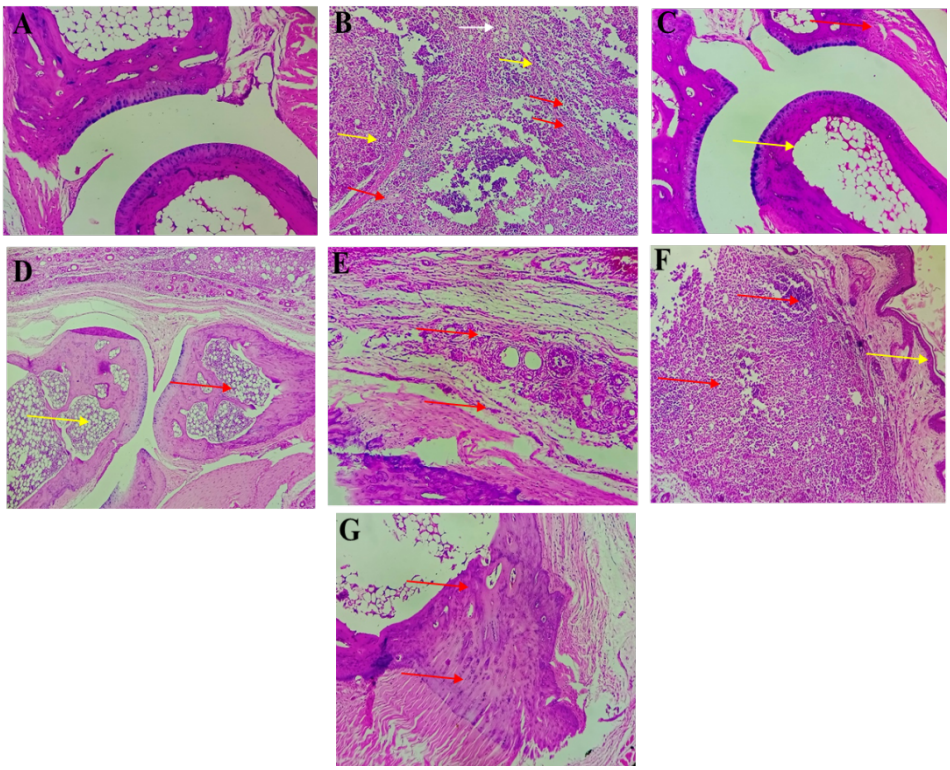

Figure 19: The following findings were obtained from a histopathological analysis of tissue with paw edema

There were no indications of inflammation in the healthy control group. Additionally, to increased inflammation, the disease control group (DC) displayed hyperaemia and congestion. Lack of synovial tissue, edema, inflammatory cell infiltration, and changes to bone and cartilage. With respect to hyperemia, edema, inflammatory cell, synovial, bone, and cartilage alterations, the Standard Control group (SC) that got Diclofenac (0.5 mg/kg, p.o.) Exhibited negligible alterations. While the B6CH group showed mild grade inflammation, hyperemia, edema, inflammatory cell infiltration, and absence of changes in synovial, bone, and cartilage changes, the BHMT group revealed only slight to moderate alterations in inflammation with decreased hyperemia, edema, and inflammatory cell infiltration—all without changing synovial, bone, or cartilage changes. In B30CH, better modifications were observed, whereas in B200CH, moderate changes were seen, including hypercellular infiltration, increased inflammatory cell presence, and the absence of synovial, bone, and cartilage alterations (as observed under H&E × 400X).

RADIOLOGICAL ANALYSIS

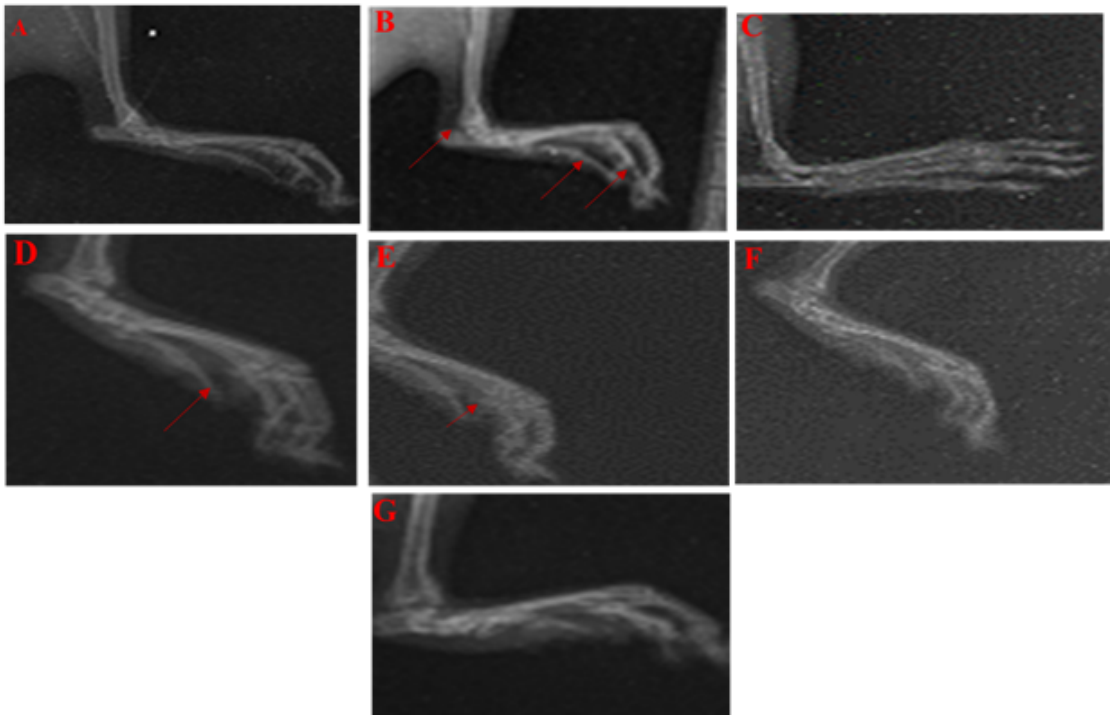

Figure 20: The following findings were obtained from a Radiological analysis of paw edema

Significant pathological changes in the CFA-induced arthritis model were revealed by an X-ray analysis of the anti-arthritis effectiveness of the selected homeopathic remedies. Group of vehicles-treated (B), rats displayed notable to severe swelling in the soft tissues surrounding the hind paw joints, accompanied by erosion near the joints and a reduction in joint space (as indicated by red arrows). Treatment using the concentrated homeopathic formulation BHMT 30C significantly reduced these arthritic changes, resulting in diminished soft tissue swelling, loss of periarticular bone, and narrowing of joint spaces in contrast to controlling group. Compared to administering the more diluted version, BHMT 6C (0.1 mL), did not produce notable anti-inflammatory effects and displayed radiological signs in to moderate arthritis observed in untreated control cases. Despite receiving 0.1 ml dilutions of BHMT, the rats showed no discernible improvement. Similar to the disease control group, these groups continued to experience mild edema and inflammation. These harmful changes were reduced when the rats were given certain homeopathic formulae, such as BHMT 200C. Compared to the untreated disease group, there was improvement in the inflammation, bone damage, and decrease in joint space.

Overall, the radiographic findings suggest that BHMT 30C, similar to the reference drug diclofenac, effectively mitigated CFA-induced inflammatory changes in the paw joints of Wistar rats, as evidenced by decreased per articular swelling, bone resorption, and joint space narrowing.

DISCUSSION

Analysis of the Bryonia alba mother tincture with HR-LCMS showed several phytoconstituents with anti-inflammatory effects. The therapeutic qualities of Bryonia alba were supported by studies that used molecular docking and MD modeling to validate the connection and elucidate the process of action between these substances and inflammatory targets linked to rheumatoid arthritis. Interestingly, the in vivo studies revealed that mice treated with Bryonia alba 30CH and 200CH formulations showed a relative better recovery, despite the limited measurable

phytochemical content, which was mainly found in the mother tincture. These findings suggest that the presence of detectable phytoconstituents might not be the sole determinant of the biological effects of potentized preparations; instead, the physical and chemical transformations occurring through repeated dilution and succussion could be equally, if not more, significant. Thus, the research indicates that the enhanced biological effect observed in potentized preparations might be linked to the phytochemical foundation of the mother tincture.

CONCLUSION

Bryonia alba mother tincture was shown to include bioactive phytoconstituents with a strong affinity for inflammatory targets using HR-LCMS profiling, molecular docking, and molecular dynamics modeling investigations. Additionally, potentized formulations, such as Bryonia alba 30CH and 200CH, exhibit notable anti-arthritic efficacy in in vivo studies. The enhanced therapeutic effect observed in potentized formulations suggests that the homeopathic potentization process might influence biological activity, despite very dilute concentrations potentially retaining only trace amounts of the original phytoconstituents. Considering all factors, the study provides comprehensive evidence of Bryonia alba formulations' anti-inflammatory and anti-arthritic effects using CFA induced arthritis. Docking, molecular dynamics and in vivo reinforcing the therapeutic potential of Bryonia alba, need of further research to elucidate the mechanisms behind potentized medications. Similar to diclofenac, BHMT 30C and 200C dramatically reduced oxidative stress, joint damage, inflammatory cytokines, and paw edema, according to in vivo investigations. As per the research, Bryonia alba exhibits promising anti-inflammatory and anti-arthritic effects.

Acknowledgement

A grant from the Dr. Babasaheb Ambedkar National Research Fellowship (BANRAF), Pune, approved by the UGC, is used to fund this work (BANRF 2021/21-22/850).

Ethics Approval Statement

The Institutional Animal Ethical Committee authorized this study (Protocol No. 2166/PO/RcBi/S/22CPCSEA).

Authors Contributions

Every author has examined and approved the completed work.

Declaration of conflict of interest

The authors certify that no identified financial conflicts of interest or personal ties had an impact on the work reported in this paper..

REFERENCES

1. Nazir S, Mobashar A, Anjum I, Chaudhary WA, Tariq N, Dar SR. Mechanistic Evaluation of Anti-Arthritic Effects of Campesterol Through Downregulation of TNF-α, IL-1β, IL-6, NF-κB, MMP 3,COX I and COX II and Upregulation of IL-4. 2023;
2. Aceves-Avila FJ, Medina F, Fraga A. The antiquity of rheumatoid arthritis: A reappraisal. J Rheumatol. 2001;28(4):751–7.
3. Ilhan M, Dereli FTG, Tümen I, Akkol EK. Anti-inflammatory and antinociceptive features of Bryonia alba L.: As a possible alternative in treating rheumatism. Open Chem. 2019;17(1):23–30.
4. Kaval I, Behçet L, Cakilcioglu U. Ethnobotanical study on medicinal plants in Geçitli and its surrounding (Hakkari-Turkey). J Ethnopharmacol. 2014;155(1):171–84.
5. Wahab S, Annadurai S, Abullais SS, Das G, Ahmad W, Ahmad F, et al. and Toxicology. Act Biol Evidence, Clin. 2021;
6. Bowers KJ, Chow E, Xu H, Dror RO, Eastwood MP, Gregersen BA, et al. Scalable algorithms for molecular dynamics simulations on commodity clusters. Proc 2006 ACM/IEEE Conf Supercomput SC'06. 2006;(May 2014).
7. Almirantis Konstantinos YT. Ultra-High Dilutions and Homeopathy: Can They Be Explained without Non-Local Theory? Homeopathy [Internet]. 2018/06/05. 2018;107(03):189–95. Available from: http://www.thieme-connect.de/products/ejournals/abstract/10.1055/s-0038-1656513
8. Yeo M. Proving the Effectiveness of Homeopathic Remedy Using a Cell-based System. Int J Clin Res Trials. 2016;1(2):1–3.
9. Bell IR. The Complexity of the Homeopathic Healing Response Part 2: The Role of the Homeopathic Simillimum as a Complex System in Initiating Recovery from Disease. Homeopathy [Internet]. 2019/11/30. 2020;109(02):51–64. Available from: http://www.thieme-connect.de/products/ejournals/abstract/10.1055/s-0039-1694999
10. Mahajan U, Walke A, Kardile M, Goyal S, Siddharth S, Kundu C, et al. Anti-inflammatory homoeopathic drug dilutions restrain lipopolysaccharide-induced release of pro-inflammatory cytokines: In vitro and in vivo evidence. Indian J Res Homoeopath. 2017;11(3):158.
11. Kristlova H. Journal of Pigmentary Disorders Melasma in Men. 2014;1(January 2015):1–4.
12. Sagar SM. Sagar-2007-Homeopathy-does-a-teaspoon-of-honey. :126–7.
13. Royal Society of Medicine (Great Britain) R. Journal of the Royal Society of Medicine. Natl Res Counc Canada - Natl Sci Libr [Internet]. 2002;95(5):221–2. Available from: https://worldwidescience.org/wws/desktop/en/service/link/track?redirectUrl
14. Saka VP, Kumar GVN, Goswami A, Sanapalli BKR,

Gupta P, Verma D, et al. Modulatory action of Bryonia alba on the immune system in cyclophosphamide induced immunosuppression in BALB/c mice. PLoS One [Internet]. 2024;19(12):1–17. Available from: http://dx.doi.org/10.1371/journal.pone.0309756

15. Leporatti ML, Ivancheva S. Preliminary comparative analysis of medicinal plants used in the traditional medicine of Bulgaria and Italy. J Ethnopharmacol. 2003;87(2–3):123–42.
16. Özüdoru B, Akaydin G, Erik S, Yesilada E. Inferences from an ethnobotanical field expedition in the selected locations of Sivas and Yozgat provinces (Turkey). J Ethnopharmacol. 2011;137(1):85–98.
17. Yeşilada E, Honda G, Sezik E, Tabata M, Fujita T, Tanaka T, et al. Traditional medicine in Turkey. V. Folk medicine in the inner Taurus Mountains. J Ethnopharmacol. 1995;46(3):133–52.
18. Garg GP, Manvi. Evaluation of Pharmacognostical parameters and Hepatoprotective activity in Bryonia alba Linn. J Chem Pharm Res. 2011;3(6):99–109.
19. Volz SM, Renner SS. Phylogeography of the ancient Eurasian medicinal plant genus Bryonia (Cucurbitaceae) inferred from nuclear and chloroplast sequences. Taxon. 2009;58(2):550–60.
20. Ielciu I, Frédérich M, Hanganu D, Angenot L, Olah NK, Ledoux A, et al. Flavonoid analysis and antioxidant activities of the bryonia alba L. Aerial parts. Antioxidants. 2019;8(4):1–11.
21. Kim S, Thiessen PA, Bolton EE, Chen J, Fu G, Gindulyte A, et al. PubChem Substance and Compound databases. 2016;44(September 2015):1202–13.
22. Eswaramoorthy, R., Hailekiros, H., Kedir, F., & Endale, M. (2021). In silico Molecular Docking, DFT Analysis and ADMET Studies of Carbazole Alkaloid and Coumarins from Roots of Clausena anisata: A Potent Inhibitor for Quorum Sensing.
23. Fernando MDM, Adhikari A, Senathilake NHKS, Silva ED de, Nanayakkara CM, Wijesundera RLC, et al. <i>In Silico</i> Pharmacological Analysis of a Potent Anti-Hepatoma Compound of Mushroom Origin and Emerging Role as an Adjuvant Drug Lead. Food Nutr Sci. 2019;10(11):1313–33.
24. Consortium TU. UniProt : a hub for protein information. 2015;43(October 2014):204–12.
25. Chr WC, Ram S, More-adate P, Tagalpallewar AA, Pawar AT, Nagar S, et al. An in-silico investigation and network pharmacology based approach to explore the anti-breast-cancer potential of Tecteria coadunata. 2023;
26. Azam SS, Abbasi SW. Molecular docking studies for the identification of novel melatoninergic inhibitors for acetylserotonin-O-methyltransferase using different docking routines. Theor Biol Med Model. 2013;10(1):1–16.
27. Rarey M, Kramer B, Lengauer T, Klebe G. A Fast Flexible Docking Method using an Incremental Construction Algorithm. 1996;470–89.
28. Chandani SR, Lokhande KB, Swamy KV, Nanda RK, Chitlange SS. Data in brief Data on docking of phytoconstituents of Actinidia deliciosa on dengue viral targets. Data Br [Internet]. 2019;25:103996. Available from: https://doi.org/10.1016/j.dib.2019.103996
29. Bowers KJ, Chow E, Xu H, Dror RO, Eastwood MP, Gregersen BA, et al. Scalable Algorithms for Molecular Dynamics Simulations on Commodity Clusters. 2006;(November).
30. Taylor P, Huang C, Li C, Choi PYK, Nandakumar K, Kostiuk LW. Molecular Physics : An International Journal at the Interface Between Chemistry and Physics A novel method for molecular dynamics simulation in the isothermal – isobaric ensemble. 2010;(August 2014):37–41.
31. Yao C, Kang Z, Yu B, Liu Y, Wang Q, Chen Q, et al. All-factor analysis and correlations on transmembrane process for arginine- rich cell penetrating peptides. 2019;
32. Harder E, Damm W, Maple J, Wu C, Reboul M, Xiang JY, et al. OPLS3 : A Force Field Providing Broad Coverage of Drug-like Small Molecules and Proteins. 2016;
33. Banks JAYL, Beard HS, Cao Y, Cho ARTE, Damm W, Farid R, et al. Integrated Modeling Program , Applied Chemical Theory (IMPACT). 2005;30580.
34. Kis L. Molecular Dynamics Simulations of Drug-Conjugated Cell-Penetrating Peptides. 2023;
35. Ivanova N, Ivanova A. Testing the Limits of Model Membrane Simulations — Bilayer Composition and Pressure Scaling. 2020;387–96.
36. Essmann U, Perera L, Berkowitz ML, Darden T, Lee H, Essmann U, et al. A smooth particle mesh Ewald method A smooth particle mesh Ewald method. 1995;8577.
37. Darden T, York D, Pedersen L. Particle mesh Ewald: An N·log(N) method for Ewald sums in large systems. J Chem Phys. 1993;98(12):10089–92.
38. Daina A, Michielin O, Zoete V. SwissADME : a free web tool to evaluate pharmacokinetics , drug-likeness and medicinal chemistry friendliness of small molecules. Nat Publ Gr. 2017;(October 2016):1–13.
39. Slater TF. [33] Overview of Methods Used for Detecting Lipid Peroxidation. Methods Enzymol.

1984;105(C):283–93.

40. Moron MS, Depierre JW, Mannervik B. Levels of glutathione, glutathione reductase and glutathione S-transferase activities in rat lung and liver. BBA - Gen Subj. 1979;582(1):67–78.

41. Misra HP, Fridovich I. The role of superoxide anion in the autoxidation of epinephrine and a simple assay for superoxide dismutase. J Biol Chem [Internet]. 1972;247(10):3170–5. Available from: http://dx.doi.org/10.1016/S0021-9258(19)45228-9

42. Aebi H. [13] Catalase in Vitro. Methods Enzymol. 1984;105(C):121–6.

43. Chandrasekar K, Subbiah P. Current Proteomics Structure-based virtual screening and molecular dynamics simulation for the identification of novel potential inhibitors for the NDM-1 of Klebsiella Pneumoniae from the marine natural products. Curr Proteomics [Internet]. 2026;23(1):100065. Available from: https://doi.org/10.1016/j.curpro.2026.100065